Research Square

Preprints are preliminary reports that have not undergone peer review.
They should not be considered conclusive, used to inform clinical practice,
or referenced by the media as validated information.

A novel Neobacillus species enhances root growth and abiotic stress tolerance in diverse host plants

Szilárd Kovács
Péter Gyula
Ágota Domonkos
Györgyi Dékány
Bilguun Tsenddorj
Orsolya Helga Jánosi
Sarolta Nagyapáti
Dima Deeb
Attila Kereszt
Gergely Maróti
Bettina Ughy
Péter Kaló

kalo.peter@brc.hu

Biological Research Centre Szeged: Szegedi Biologiai Kutatokozpontja https://orcid.org/0000-0002-0404-8904

Research Article

Keywords: Plant Growth Promoting Rhizobacteria, Solanum lycopersicum, Medicago truncatula, Biofilms, auxin, Salt stress

Posted Date: November 18th, 2026

DOI: https://doi.org/10.21203/rs.3.rs-11431330/v1

License: This work is licensed under a Creative Commons Attribution 4.0 International License.
Read Full License

A novel *Neobacillus* species enhances root growth and abiotic stress tolerance in diverse host plants

Szilárd Kovács[1]*, Péter Gyula[1], Ágota Domonkos[2], Györgyi Dékány[1], Bilguun Tsenddorj[1,3], Orsolya Helga Jánosi[1], Sarolta Nagyapáti[1], Dima Deeb[1], Attila Kereszt[1], Gergely Maróti[1], Bettina Ughy[1], Péter Kaló[1,2]*

[1] Institute of Plant Biology, HUN-REN Biological Research Centre, Szeged, Hungary

[2] Institute of Genetics and Biotechnology, Hungarian University of Agriculture and Life Sciences, Gödöllő, Hungary

[3] Doctoral School of Biology, Faculty of Science and Informatics, University of Szeged, Szeged, Hungary

* Corresponding authors: Péter Kaló (kalo.peter@brc.hu), Szilárd Kovács (kovacs.szilard@brc.hu)

ORCID IDs:

Szilárd Kovács: 0009-0002-6730-567X

Péter Gyula: 0000-0002-3574-2827

Ágota Domonkos: 0000-0003-4017-0605

Bilguun Tsenddorj: 0000-0003-3942-1403

Dima Deeb: 0000-0003-0448-9926

Attila Kereszt: 0000-0002-4421-6554

Gergely Maróti: 0000-0002-3705-0461

László Szilák: 0000-0003-0334-272X

Bettina Ughy: 0000-0002-8030-9950

Péter Kaló: 0000-0002-0404-8904

Keywords

Plant Growth Promoting Rhizobacteria; Solanum lycopersicum; Medicago truncatula; Biofilms; auxin; Salt stress

Abstract

Background and aims

Plant growth-promoting rhizobacteria (PGPR) offer a sustainable approach to improving plant performance and mitigating the effects of abiotic stress. In this study, we investigated the root-associated bacterial communities in greenhouse-grown, non-symbiotic *Medicago truncatula* and isolated *Neobacillus* sp. B4567, a previously uncharacterized endophytic strain. We characterized the genome sequencing, and growth promoting potential in plant species and evaluated its effects on tomato under drought and salinity stress.

Methods

Whole-genome comparative phylogenomic analyses were performed to determine the taxonomic position of strain B4567. In vitro assays assessed its plant growth-promoting traits and tolerance to osmotic and salinity stress. The growth-promoting effects were evaluated in multiple plant species, while root architecture and performance was analyzed in tomato under soil-based drought and salinity stress.

Results

Phylogenomic analyses identified B4567 as a distinct species within the genus *Neobacillus*. The strain B4567 produced indole-3-acetic acid (IAA), tolerated osmotic and saline stress, and formed robust biofilms *in vitro*. Inoculation promoted biomass accumulation in all tested plant species. In tomato, growth stimulation was associated with increased secondary lateral root proliferation. Under drought and salinity stress conditions, B4567-inoculated tomato plants exhibited vegetative growth, earlier flowering and fruit ripening, and significantly increased total fruit yield.

Conclusion

Neobacillus sp. B4567 is a novel, promising bioinoculant with broad-host growth-promoting activity and the potential to improve plant productivity under drought and salinity stress. The combination of its plant growth-promoting traits and environmental stress tolerance makes it a promising candidate for further development for sustainable agriculture.

Introduction

Plant-growth-promoting rhizobacteria (PGPR) inhabit the rhizosphere or colonize plant roots, where they can directly or indirectly influence plant growth and development. Owing to their beneficial effects on plants, PGPRs have long been the focus of extensive research (Kloepper 1978; Lugtenberg and Kamilova 2009; Yang et al. 2009; Ryu et al. 2024) and are increasingly recognized as environmentally friendly and sustainable tools that may help reduce the reliance on chemical fertilizers (Shahwar et al. 2023; He et al. 2024). These bacteria promote plant growth through diverse mechanisms, including enhancing nutrient availability and uptake, stimulating root growth, improving soil structure, strengthening plant immunity, and contributing to the decomposition of soil organic matter (Rosier et al. 2018; Irfan et al. 2026). Among these effects, the modulation of root system architecture (RSA) is particularly important because roots are the primary organs responsible for water and nutrient uptake and serve as the main interface between plants and soil microorganisms.

PGPRs can modify RSA by influencing the number, length, and spatial distribution of primary and lateral roots. These effects can be mediated by several mechanisms, including the production of phytohormones such as auxins, cytokinins, and gibberellins. In addition, some PGPRs influence root growth by modulating ethylene homeostasis by the activity of 1-aminocyclopropane-1-carboxylate (ACC) deaminase. This enzyme cleaves ACC, the immediate precursor of ethylene, thereby reducing ethylene levels in plant tissues and potentially alleviating ethylene-mediated inhibition of root growth. Root architecture is also strongly influenced by external nutrient availability which acts as an environmental signal to regulate RSA (Giehl et al. 2014).

Changes in RSA can contribute to plant resilience under drought and salinity stress by modifying root distribution and increasing the effective volume of soil explored for water and nutrient acquisition. Under saline conditions, changes in root architecture may also improve access to water and essential nutrients, thereby helping plants cope with the adverse effects of salinity. Beyond their effects on root morphology, PGPR-mediated changes in phytohormone homeostasis can influence root exudation, potentially facilitating the recruitment of additional beneficial microorganisms and shaping the rhizosphere microbial community. PGPRs may also alter plant metabolic pathways and carbon allocation between shoots and roots, favoring root growth and development under stress conditions. Collectively, these processes can improve

resource acquisition and contribute to plant adaptation to challenging environmental conditions (Zerrouk et al. 2016; Jochum et al. 2019; Zhao et al. 2023).

Auxins play crucial roles in numerous aspects of plant development, including shoot and leaf growth by stimulation of cell elongation, the regulation of apical dominance, and the promotion of fruit development (Pattison et al. 2014; Zhao 2018). Among their diverse functions, auxins are particularly important for RSA, where they promote lateral root formation and regulate primary root elongation in a concentration-dependent manner, resulting in a bimodal response (Overvoorde et al. 2010). Microbially produced auxins released into the rhizosphere can be taken up by plants and contribute to the endogenous auxin pool, thereby influencing auxin distribution and signaling in the root. Consequently, microbial auxins can affect multiple stages of lateral root development, including lateral root initiation, emergence, and subsequent elongation (Moharana et al. 2026).

Species of the genus *Neobacillus*, which includes taxa previously assigned to *Bacillus* and related lineages, have recently attracted attention as potential PGPRs because of their environmental resilience, spore-forming capacity, and diverse functional traits (Kämpfer et al. 2022; Han et al. 2023). Several *Neobacillus* isolates have demonstrated plant growth-promoting properties (Martínez-Hidalgo et al. 2021); with some strains exhibiting indole-3-acetic acid (IAA) production, ACC deaminase activity and the ability to modulate plant-microbe interactions (Bhattacharjee et al. 2023). These traits may influence RSA and promote plant growth, highlighting the potential of *Neobacillus* species as bioinoculants for sustainable agriculture.

In this study, we report the isolation and characterization of a novel *Neobacillus* sp. strain that promotes root growth and biomass accumulation in several plant species, including *Medicago truncatula*, *Solanum lycopersicum* (tomato), *Brachypodium distachyon*, and *Nicotiana benthamiana*. Inoculation with this strain alters RSA, as evidenced by increased lateral root proliferation and enhances overall plant biomass compared with uninoculated controls. The strain produces auxin-related compounds, forms biofilms, and exhibits tolerance to osmotic and saline stress. These characteristics may contribute to its growth-promoting effects in different host species and under varying environmental conditions. Collectively, our findings identify this newly characterized *Neobacillus* sp. strain as a promising multifunctional PGPR and highlight its potential for use in sustainable cropping systems, particularly under abiotic stress conditions.

Materials and Methods

Plant material, bacterial inoculation, and growth conditions

Medicago truncatula Jemalong A17*, Brachypodium distachyon* Bd21 inbred line (Garvin et al. 2008), *Nicotiana benthamiana*, and *Solanum lycopersicum* cv. Vilma were used in this study. Seeds were surface sterilized with 10% hypochlorite solution for 3 min and subsequently washed thoroughly with sterile distilled water. Before sterilization, *M. truncatula* seeds were scarified using sandpaper. Following sterilization, seeds were imbibed in water for approximately 3 h at 4 °C. They were then transferred to pots 250-mL pots containing either zeolite (Geoproduct Kft., Mád, Hungary or vermiculite, or to 1-L pots containing a soil-sand mixture. Plants were grown in a greenhouse at 22–26 °C under a 16 h light, 8 h dark photoperiod. Plants were watered once a week with Fåhræus medium (Barker et al. 2006) supplemented with 2.5 mM NH_4NO_3 and 2 mM KNO_3.

For bacterial inoculation, strains were grown in TY+Ca agar medium (3 g L^{-1} yeast extract, 5 g L^{-1} Tryptone N1 supplemented with 6 mM $CaCl_2$) at 30 °C for 3 days. Bacterial cells were harvested and resuspended in Fåhræus medium supplemented with 2.5 mM NH_4NO_3 and 2 mM KNO_3, and the suspension was adjusted to OD_{600} = 0.1. For experiments carried out in 250-mL pots, five-day-old seedlings were inoculated with 20 mL of a bacterial suspension. In drought- and salinity-stress experiments conducted in 1-L pots containing a soil–sand mixture, 20 mL of a bacterial suspension was applied to the root zone of each plant at 0 and 14 days after sowing. Control plants received an equivalent volume of Fåhræus medium.

Isolation of plant growth promoting (PGP) bacterial strains

Wild-type *Medicago truncatula* Jemalong plants were grown in zeolite substrate soaked with Fåhræus medium supplemented with 2.5 mM NH_4NO_3 and 2 mM KNO_3. Plants were maintained under greenhouse conditions and watered with distilled water, while nitrogen-containing Fåhræus medium was supplied once a week. Root segments were collected from six-week-old plants and surface-sterilized by immersion in 70% ethanol for 5 min, followed by three 5-min washing steps with Milli-Q water. The sterilized root segments were then homogenized in 0.9% NaCl solution using a sterile glass pestle. To remove debris, the homogenates were briefly spun down for a few seconds, and the resulting supernatants were transferred to fresh tubes. Serial dilutions (10^{-1}, 10^{-2}, 10^{-3}) were prepared from the supernatants, and 100 µL of each dilution was plated onto TY+Ca agar plates. The plates were incubated at

30 °C for 3 days, after which distinct bacterial morphotypes were distinguished based on colony morphology.

Genome sequencing, assembly, and annotation

To obtain a complete genome of the isolate, both long-read and short-read technologies were employed. Long-read sequencing was performed by Novogene (Cambridge, UK) using the Oxford Nanopore Technologies (ONT, Oxford, UK) PromethION platform. Real-time base calling and demultiplexing were performed using the High Accuracy model (dna_r10.4.1_e8.2_400bps_hac@v5.0.0). In total, 748,746 quality-filtered reads were obtained, with a mean read length of 3,893.7. The mean read quality was 15.6, and the read length N50 was 6,044. Short-read sequencing libraries were prepared and sequenced by mBioWorks (Copenhagen, Denmark) on MGISEQ-2000 platform (MGI Tech Co., Ltd., Shenzhen, China) using 2×150 bp chemistry. Raw reads were trimmed and quality-filtered using fastp (v0.20.1) (Chen et al. 2018). After processing, 7,340,515 clean read pairs were retained with a mean size of 137 bp and a mean insert size of 269 bp. The percentage of Q30 bases was 96.6%.

Genome assembly was performed using Trycycler (v0.5.6) (Wick et al. 2021). The resulting circular sequences were first corrected with the long-read polisher Medaka (v2.2.2) using the quality-filtered long reads, and then subsequently polished with Polypolish (v0.6.1) using the quality-filtered short reads (Wick and Holt 2022). The completeness of the assemblies was assessed using BUSCO and CheckM2 (Chklovski et al. 2023; Tegenfeldt et al. 2025), which estimated genome completeness at 99.5% and 100%, respectively. The final genome assembly was annotated using the NCBI Prokaryotic Genome Annotation Pipeline (Tatusova et al. 2016). The assembled genome and the raw sequencing reads were deposited in the NCBI database under BioProject accession number PRJNA1516868.

Taxonomic analysis

For the 16S rRNA-based phylogenetic tree construction, the 15 copies of the 16S rRNA gene identified in the annotated genome were first retrieved, and their sequence similarities were assessed by multiple sequence alignment using MUSCLE (v3.8.1551) (Edgar 2004), followed by constructing a neighbor-joining phylogenetic tree. The least divergent 16S rRNA sequence was selected for further analysis (locus tag: AC7SJ9_00150). This sequence was used to perform a BLAST search against the NCBI 16S rRNA database restricted to type material. The sequences corresponding to representative members of various genera within the *Bacillaceae*

family were retrieved; *Staphylococcus aureus* strain ATCC 12600 was included as an outgroup. The selected sequences were aligned using MUSCLE, and a phylogenetic tree was constructed using the Maximum Likelihood method with MEGA 11 software (Tamura et al. 2021). Nucleotide substitutions were modeled using the General Time Reversible (GTR) model. Evolutionary rate differences among sites were modeled with a discrete Gamma distribution across five categories (+G), allowing for evolutionarily invariant sites (+I). The partial deletion option was applied to eliminate positions with less than 95% site coverage. The robustness of the tree topology was evaluated using a bootstrap method with 1,000 replicates.

Ribosomal Multilocus Sequence Typing was performed using the PubMLST server (Jolley et al. 2018) which compared 53 genes encoding bacterial ribosomal protein subunits (*rps* genes) against the database. For genome-scale taxonomic assignment, the closest bacterial genomes were determined with the Type Strain Genome Server (Meier-Kolthoff et al. 2022). Pairwise Average Nucleotide Identity by BLAST (ANIb) values were calculated using the JSpeciesWS server (Richter et al. 2016).

Pathway reconstruction

For metabolic pathway reconstruction, the predicted protein sequences of strain B4567 were annotated against the eggNOG 7 database using the eggNOG-mapper v3 server (Hernández-Plaza et al. 2026) to assign KEGG Orthology (KO) identifiers. These KO numbers were then submitted to the KEGG Mapper Reconstruct tool (Kanehisa et al. 2022) to reconstruct and visualize the metabolic pathways. Predicted enzymes are highlighted in green on the resulting pathway maps.

Phosphate solubilization assay

The phosphate-solubilizing ability of the bacterial strain was assessed on Pikovskaya agar plates containing 10 g L^{-1} glucose, 5 g L^{-1} $Ca_3(PO_4)_2$, 0.5 g L^{-1} $(NH_4)_2SO_4$, 0.1 g L^{-1} $MgSO_4 \cdot 7H_2O$, 0.2 g L^{-1} KCl, 0.5 g L^{-1} yeast extract, 0.001 g L^{-1} $MnSO_4 \cdot H_2O$, and 0.001 g L^{-1} $FeSO_4 \cdot 7H_2O$ (Pikovskaya 1948). Plates were incubated at room temperature for one week. Phosphate solubilization was assessed by the formation of clear halo zones surrounding bacterial colonies.

Siderophore production assay

Siderophore production by the bacterial strain was assessed using blue agar plates containing the chrome azurol S (CAS)/iron(III)/hexadecyltrimethylammonium bromide (HDTMA) complex as an indicator. The indicator solution was prepared by dissolving 60.5 mg CAS in 50 ml distilled water and mixing it with 10 ml of an iron(III) solution containing 1 mM $FeCl_3 \cdot 6H_2O$ in 10 mM HCl. This mixture was slowly added to 40 ml of an HDTMA solution prepared by dissolving 72.9 mg HDTMA with continuous stirring. Following autoclaving, the indicator solution was added to the growth medium at a final concentration of 10% (v/v). Siderophore production was indicated by a color change of the medium from blue to orange. Plates were incubated at room temperature for one week before evaluation.

Auxin-related compound production assay

The production of auxin-related compounds was evaluated using a modified colorimetric Salkowski assay (Salkowski 1885). Bacterial cultures were grown in YMA medium containing 0.2 g L^{-1} K_2HPO_4, 0.2 g L^{-1} $MgSO_4 \cdot 7H_2O$, 10 g L^{-1} Mannitol, 0.3 g L^{-1} yeast extract, 0.05 g L^{-1} NaCl (pH 7.0), with or without tryptophan supplementation (1 g L^{-1}) Following incubation, cultures were centrifuged, and the resulting supernatant was mixed with the Salkowski reagent, consisting of 35% concentrated H_2SO_4 and 0.0098 M $FeCl_3$, at a sample-to-reagent ratio of 1:2. Absorbance was measured at 530 nm using a Hidex Sense Microplate Reader (Hidex, Turku, Finland) equipped with Plate Reader Software version 5064. The concentration of Salkowski-reactive auxin-related compounds was estimated from a calibration curve generated using indole-3-acetic acid (IAA standards (Sigma-Aldrich, USA), at concentrations ranging from 12.5 to 50 µg/mL.

ACC deaminase activity assay

The ACC deaminase activity of the bacterial strain was assessed using Dworkin-Foster (DF) medium (Dworkin and Foster 1958) containing 3 mM 1-aminocyclopropane-1-carboxylic acid (ACC) as the sole nitrogen source. The DF medium contained 4 g L^{-1} KH_2PO_4, 6 g L^{-1} Na_2HPO_4, 0.2 g L^{-1} $MgSO_4 \cdot 7H_2O$, 2 g L^{-1} glucose, 2 g L^{-1} gluconic acid, and 2 g L^{-1} citric acid, supplemented with trace elements (1 mg L^{-1} $FeSO_4 \cdot 7H_2O$, 10 mg L^{-1} H_3BO_3, 11.19 mg L^{-1} $MnSO_4 \cdot H_2O$, 124.6 mg L^{-1} $ZnSO_4 \cdot 7H_2O$, 78.22 mg L^{-1} $CuSO_4 \cdot 5H_2O$, and 10 mg L^{-1} MoO_3). In control cultures, $(NH_4)_2SO_4$ was used as the nitrogen source. Growth was assessed after 1, 2,

and 3 days of incubation by measuring culture density at OD_{600} and comparing growth in ACC-containing medium with that of the control cultures.

Osmotic and salinity stress tolerance assays

To assess osmotic and salinity stress tolerance, bacterial strain was grown overnight in TY+Ca medium at 30 °C with shaking. The overnight culture was then diluted in TY+Ca medium or TY+Ca medium supplemented with 10, 20, or 30% (w/v) polyethylene glycol 6000 (PEG-6000), or 5, 10 or 15% (w/v) NaCl to an initial OD_{600} of 0.05. A volume of 300 µL of each bacterial suspension was transferred to a 96-well Microtest plate (Sarstedt REF 82.1581001). Bacterial growth kinetics were monitored using a Hidex Sense Microplate Reader (Hidex, Turku, Finland) equipped with Plate Reader Software version 5064.

Biofilm formation under osmotic and salinity stress

To assess biofilm formation of the bacterial strain and determine the effects of osmotic and salinity stress on biofilm formation, the strain was grown overnight in TY+Ca medium at 30 °C with shaking. Cultures were subsequently diluted in TY+Ca medium or TY+Ca medium supplemented with 10, 20, or 30% (w/v) PEG-6000 and 5, 10 or 15% (w/v) NaCl, to an initial OD_{600} of 0.1. Cultures were incubated for 4–6 days at 30 °C with shaking to allow biofilm formation. Following incubation, the 3 ml culture was discarded from each tube, and the tubes were washed three times with distilled water (DW) to remove remaining cells. Biofilms attached to the tube surface were stained with 10 ml of 0.1% (w/v) crystal violet solution for 10 min at room temperature. Crystal violet solution was subsequently removed, and the tubes were washed three times with DW. Stained biofilms were dried overnight at room temperature and then visualized. The bound crystal violet was subsequently solubilized by adding 2 ml 96% acetic acid and mixed thoroughly. Biofilm mass was quantified by measuring absorbance at 570 nm using a Hidex Sense Microplate Reader.

Germination test

To evaluate whether the bacteria influence seed germination, sterilized tomato seeds were put on sterilized filter paper soaked with half-strength Murashige and Skoog (½ MS) medium either without bacteria or supplemented with a bacterial suspension adjusted to an OD_{600} of 0.1 for 7 days.

Experimental design for drought and salinity stress

Drought and salinity stress experiments were conducted under greenhouse conditions. Tomato plants were grown in a 1:1 (v/v) soil-sand mixture. To determine the water-holding capacity of the growth substrate, the soil-sand mixture was completely dried, and an amount corresponding to the volume of one pot was weighed. The substrate was then fully saturated with distilled water and weighed again. The difference between the dry and saturated weights was used to determine the water-holding capacity. Soil water content was subsequently maintained at 80% of the water-holding capacity under control conditions. For the drought treatment, soil water content was gradually reduced to 30% beginning 30 days after sowing. Pots were weighed daily, and the required amount of water was added to maintain the target soil water content at 80% under control conditions and 30% under drought stress conditions.

For the salinity treatment, the dried soil-sand mixture was fully saturated with a 50 mM NaCl solution, and the soil water content was subsequently adjusted to 80% of the water-holding capacity. Pots were weighed daily, and the required amount of the corresponding solution was added to maintain the soil water content at 80% throughout the experiment under both control and salinity conditions.

Measuring photosynthetic activity

Chlorophyll *a* fluorescence induction kinetics were measured using a Handy-PEA fluorometer (Hansatech Instruments Ltd., Serial No. 2646, UK). Before measurements, tomato plants were dark-adapted for 50 min to ensure that the photosynthetic apparatus reached a stable dark-adapted state. Immediately after dark adaptation, lightweight plastic leaf clips equipped with sliding shutter plates, supplied with the instrument, were attached to the selected leaves. This procedure was performed in a dark room under dim green light to minimize exposure to actinic radiation.

Measurements were taken sequentially, starting with the lowest selected leaves and proceeding upwards; basal leaves located closest to the soil surface were excluded. Three leaves were measured per plant, with one measurement point recorded per leaf. Each leaf was exposed to a continuous, high-intensity red light pulse of 3500 μmol m^{-2} s^{-1} for 5.0 s, generated by an array of three high-output light-emitting diodes with a peak wavelength approximately 650 nm.

The minimum fluorescence (F_0), maximum fluorescence (F_m), variable fluorescence (F_v), and maximum quantum efficiency of photosystem II (F_v/F_m) were recorded and calculated using the integrated PEA Plus software. These parameters were used to assess the photochemical efficiency and functional status of photosystem II in the tomato leaves.

Statistical analyses

To evaluate the effect of bacterial treatment on plant traits, statistical comparisons were performed according to the experimental design. For comparison between two groups, two-tailed unpaired *t*-tests were used. For experiments involving treatment and environmental-conditioning factors, data were analyzed by two-way ANOVA followed by Duncan's post hoc test. When multiple treatment groups were compared with a mock-inoculated control, one-way ANOVA followed by Dunnett's post hoc test was used. For time-course measurements of photosynthetic efficiency (F_v/F_m), a generalized linear mixed-effects model with a beta distribution and logit link function was fitted. Effects and interactions were evaluated using Wald chi-square tests, followed by Tukey's post hoc tests. Data are presented as mean ± standard error (*SE*). Statistical significance was thresholded at $p < 0.05$ (* $p < 0.05$, ** $p < 0.01$, *** $p < 0.001$. Adjusted *p*-values were reported where post hoc corrections were applied.

Results

Bacterial isolation and identification from *Medicago truncatula* roots

To investigate the endophytic bacterial communities associated with *Medicago truncatula* roots under non-symbiotic greenhouse conditions, bacterial isolates were obtained from wild-type *M. truncatula* Jemalong plants. Following surface sterilization, root samples were processed to isolate endophytic bacteria by cultivation on TY+Ca agar plates. The resulting bacterial communities were subcultured and subsequently used to inoculate *M. truncatula* roots. Four weeks after inoculation, shoot and root dry weights were determined and compared with those of uninoculated control plants (Fig. 1A). Inoculation with one bacterial mixture, designated "9" significantly increased plant biomass relative to the mock-inoculated controls (Fig. 1B).

To identify the bacterial strain(s) responsible for the observed growth-promoting effect, roots of *M. truncatula* plants inoculated with the mixture "9" were surface-sterilized, homogenized, and plated on TY+Ca agar to recover root-associated bacteria. Based on colony morphology, six distinct bacterial isolates were recovered from the root tissues (Fig. S1). Each isolate was subsequently purified and individually re-inoculated onto *M. truncatula* roots. Of

the six isolates tested, only one, designated “9.6”, significantly promoted plant growth (Fig. S1D and E; Fig. S1F).

Genome sequencing and taxonomic classification of the plant-growth-promoting isolate

To determine the precise phylogenetic position of the isolate, its genome was sequenced using a hybrid approach combining long- and short-read sequencing technologies. The genome was assembled into two complete, circular replicons: a 5,923,201-bp chromosome with a G+C content of 38.7% and a 172,124-bp megaplasmid with a G+C content of 35.8%. The chromosome and megaplasmid were predicted to encode 5,663 and 162 protein-coding genes, respectively. The genome also contained 15 copies of the ribosomal RNA (rRNA) operon, a genomic feature that has been associated with enhanced growth potential and adaptation to changing environmental conditions (Klappenbach et al. 2000).

The overall genome size is consistent with that of free-living bacteria, whereas the relatively low G+C content is more characteristic of obligatory pathogens and symbionts. Furthermore, the lower G+C content of the megaplasmid compared with the chromosome may indicate that the megaplasmid was acquired by horizontal gene transfer (Mann and Chen 2010). Consistent with this possibility, the megaplasmid contains genes associated with conjugation, replication, and sporulation, as well as genes involved in formaldehyde and reactive oxygen species (ROS) detoxification and alternative nitrogen utilization. Genome-based pathogenicity prediction classified the strain as a “Human Non-Pathogen” with a probability score of 0.0809, substantially below the predefined pathogenicity threshold of 0.5.

Taxonomic classification of the isolate was performed in multiple steps. First, genus-level assignment was based on phylogenetic analysis of the 16S rRNA gene sequence, which placed the isolate within the genus *Neobacillus* (Fig. 2A).

Subsequent species-level identification using ribosomal multilocus sequence typing (rMLST) indicated that the strain was most closely related to *Neobacillus drentensis*. To obtain a more comprehensive, genome-scale assessment of its taxonomic position, the closest genomic relatives were identified using the Type Strain Genome Server (TYGS) (Meier-Kolthoff et al. 2022). The highest digital DNA–DNA hybridization (dDDH) values were obtained for *Neobacillus nitrireducens* and *Neobacillus drentensis*, with values of only 27.2% and 26.7%, respectively. These values are substantially below the generally accepted threshold of ≥70%

dDDH for species delineation (Goris et al. 2007; Meier-Kolthoff et al. 2014), strongly supporting the hypothesis that the isolate represents a novel *Neobacillus* species.

To further assess the taxonomic distinctiveness of the isolate, Average Nucleotide Identity based on BLAST (ANIb) was calculated against the same closely related genomes. ANIb values of 81.95% and 81.67% were obtained for *N. nitrireducens* and *N. drentensis*, respectively, with corresponding alignment rates of 54.18% and 51.90%. Both ANI values are well below the widely accepted species delineation threshold of approximately 95% ANI (Goris et al. 2007). The combination of low ANI values and relatively low genome alignment rates provides additional evidence that the isolate represents a genetically distinct and previously undescribed species within the genus *Neobacillus*. To further investigate the evolutionary relationship of the isolate to other members of the genus, a whole-genome-based phylogenetic tree was constructed, including the *Neobacillus* sp. strain isolated in this study and representative *Neobacillus* genomes (Fig. 2B).

Taken together, these analyses indicate that the isolate shares a conserved genomic backbone with members of the *Neobacillus drentensis* lineage while exhibiting sufficient genomic divergence to distinguish it from currently described species. Accordingly, we propose that the isolate represents a novel species within the genus *Neobacillus* and designate it *Neobacillus* sp. strain B4567.

Neobacillus sp. strain B4567 promotes root growth in crop and model plants

To assess the broader plant growth-promoting potential of *Neobacillus* sp. strain B4567, we inoculated two additional model plants, *Brachypodium distachyon* and *Nicotiana benthamiana*, and the crop plant *Solanum lycopersicum* with the isolate. Plants were grown for four weeks, after which shoot and root dry weights were determined and compared with those of mock-inoculated controls. Representative images of mock-inoculated and B4567-inoculated *S. lycopersicum* (Fig. 3A), *B. distachyon* (Fig. 3B), and *N. benthamiana* (Fig. 3C) plants illustrate the growth-promoting effect of *Neobacillus* sp. strain B4567. Quantification of shoot and root dry weights (Fig. 3D–F) revealed a significant increase in biomass following inoculation across all three host species. Notably, the increase in root biomass was more pronounced than that of the shoot biomass, suggesting that stimulation of root growth may represent a major component of the growth-promoting effect of *Neobacillus* sp. strain B4567.

Across the tested host species, the root biomass accounted for a disproportionate share of the overall increase in biomass, suggesting that the stimulation of root development may represent a primary component of the growth-promoting effect of the strain. To further validate this observation, we monitored the growth kinetics of tomato plants following inoculation and compared the dry weights of root and shoot tissues with mock-inoculated controls at multiple time points. Representative images of tomato plants collected between 0 and 18 days post-inoculation (dpi) revealed a pronounced early increase in root biomass in inoculated plants, evident as early as 4 dpi (Fig. S2). Quantitative measurements of dry weight confirmed that root biomass was significantly higher in B4567-inoculated plants than in mock-inoculated controls from 4 dpi onward (Fig. 4A). The increase in root biomass persisted throughout the experimental period, whereas shoot biomass remained comparable to that of mock-inoculated controls until 10 dpi (Fig. 4A–B). By 18 dpi, both root and shoot dry weights were significantly higher in B4567-inoculated plants, demonstrating a sustained growth-promoting effect on overall plant biomass (Fig. 4A–B).

To determine whether the root-biased growth response observed in the kinetic experiment was associated with changes in root system architecture, we quantified lateral root formation in tomato plants at 14 dpi with *Neobacillus* sp. strain B4567. We quantified two classes of lateral roots: (i) primary lateral roots emerging directly from the primary root and (ii) secondary lateral roots emerging from primary lateral roots. Inoculation with *Neobacillus sp.* strain B4567 did not significantly affect the number of primary lateral roots compared to mock-inoculated controls. In contrast, the number of secondary lateral roots was significantly increased in plants inoculated with *Neobacillus* sp. strain B4567 (Fig. 5, Fig. S3).

The absence of a detectable effect on primary lateral root formation may be attributable to the timing of bacterial inoculation. At the time of inoculation, the first primary lateral root primordia had already been initiated and were emerging from the primary root, leaving a limited window during which bacterial treatment could influence subsequent primary lateral root initiation. In contrast, the increase in secondary lateral root formation is consistent with the early, root-biased increase in biomass observed in the kinetic experiment (Fig. 4A), suggesting that B4567 preferentially promotes the development of higher-order lateral roots.

Characterization of plant growth-promoting traits of *Neobacillus* sp. strain B4567

To gain insight into the mechanisms underlying the growth- and root architecture-promoting phenotypes observed in tomato, *B. distachion*, *N. benthamiana*, and *M. truncatula*, we

characterized the plant growth-promoting trait profile of *Neobacillus* sp. strain B4567 under controlled *in vitro* conditions. The strain was tested for inorganic phosphate solubilization on Pikovskaya agar, siderophore production using CAS agar, auxin production, and ACC (1-aminocyclopropane-1-carboxylate) deaminase activity. In addition, tolerance to osmotic and salinity stress was evaluated using liquid growth kinetics assays, and biofilm formation was assessed under the same stress conditions.

No transparent halo zones were detected around colonies on the Pikovskaya agar, indicating that the isolate did not exhibit detectable inorganic phosphate solubilization under the tested conditions. Similarly, no color change was observed in the Blue Agar CAS assay, indicating an absence of detectable siderophore production. ACC deaminase activity was also not detected under the conditions tested. Consistent with this result, genome sequence analysis of strain B4567 did not identify the canonical *acsdS* gene encoding ACC deaminase, further supporting the absence of detectable ACC deaminase activity in this strain.

Production of auxin-related compounds

The production of auxin-related compounds by *Neobacillus* sp. strain B4567 was assessed using the Salkowski assay. The strain was grown in either mock or tryptophan-supplemented liquid YMA medium, and samples were collected after 24 or 48 h. In both media, bacterial cultures reached the stationary phase after 24 h and entered the decline phase by 48 h (Fig. 6A). Cell-free supernatants collected at both time points were subsequently analyzed using the Salkowski assay. A strong purple coloration was observed only in supernatants from cultures grown in tryptophan-supplemented medium. Absorbance was measured spectrophotometrically at 530 nm using a Hidex Sense Microplate Reader (Fig. 6B). Auxin-related compound concentrations were estimated by comparing OD_{530} values with a calibration curve generated using IAA standards. *Neobacillus* sp. strain B4567 produced 19.5 µg/ml and 10.5 µg/ml of IAA-equivalent compounds after 24 and 48 h of incubation, respectively (Fig. 6C).

To identify potential genetic pathways underlying auxin biosynthesis, the predicted protein sequences of strain B4567 were analyzed against the eggNOG 7 database. Pathway reconstruction identified genes associated with putative IAA biosynthetic routes involving tryptamine (TAM) and indole-3-acetamide (IAM) intermediates (Fig. S5).

Together, these results suggest that inorganic phosphate solubilization, siderophore production, and ACC deaminase activity are unlikely to represent the major plant growth-

promoting traits of *Neobacillus* sp. strain B4567. In contrast, the strain exhibited detectable auxin production (Table 1, Fig. 6), suggesting that this trait may contribute to its plant growth-promoting activity.

Stress tolerance and biofilm formation under osmotic and salinity stress

To characterize the growth kinetics of *Neobacillus* sp. strain B4567 under control and stress conditions, bacterial growth was monitored for 72 h. In standard TY+Ca medium, the strain reached the stationary phase at approximately 48 h post-inoculation (Fig. 7A and C).

Under osmotic stress, increasing concentrations of PEG-6000 (10%, 20%, and 30%) progressively impaired bacterial growth. At 10% PEG, the strain displayed robust growth and reached the stationary phase earlier than in the control medium. In contrast, growth was strongly reduced in the presence of 20% PEG, while no detectable growth was observed at 30% PEG (Fig. 7A). Viability assays performed after 72 h confirmed that cells exposed to 30% PEG were no longer viable (Fig. 7B). These results indicate that *Neobacillus* sp. strain B4567 tolerates osmotic stress up to 20% PEG, whereas 30% PEG represents a non-permissive condition under the conditions tested.

Under salinity stress, supplementation with 5%, 10%, or 15% NaCl resulted in relatively minor changes in the overall growth profile. Increasing NaCl concentrations primarily led to a gradual extension of the lag phase, whereas the subsequent growth phases remained largely comparable to those observed in the control medium (Fig. 7C). Consistent with these observations, viable cells were detected after 72 h under all tested NaCl concentrations (Fig. 7B). These results indicate that *Neobacillus* sp. strain B4567 retains viability and the capacity for growth under relatively high salinity conditions.

We next assessed the ability of strain B4567 to form biofilms under control and stress conditions. In standard TY+Ca medium, the strain exhibited moderate biofilm formation after 4 days, which increased to high levels after 6 days of incubation (Fig. 7D; Fig. S4). Based on these observations, biofilm formation under stress conditions was quantified after 6 days of incubation. Under osmotic stress, biofilm formation was detected in the presence of 20% PEG, despite the strongly reduced growth observed under this condition (Fig. 7A and D; Fig. S4). Under salinity stress, biofilm formation was detected in the presence of 5% NaCl but was strongly reduced or absent at higher NaCl concentrations (Fig. 7D; Fig. S4). Together, these results indicate that B4567 retains the capacity to form biofilms under selected osmotic and

salinity stress conditions, although biofilm formation is progressively impaired at higher stress levels.

Evaluation of the plant growth-promoting potential of *Neobacillus* sp. strain B4567 under normal and abiotic stress conditions

To assess the potential application of *Neobacillus* sp. strain B4567, we investigated its effects on seed germination and early root development, as well as on plant growth, flowering, fruit ripening, and yield of tomato plants grown in soil under normal conditions and exposed to salinity or drought stress.

To determine the effect of *Neobacillus* sp. strain B4567 on tomato seed germination, seeds were germinated on half-strength Murashige and Skoog (½ MS) medium either without bacteria or supplemented with a bacterial suspension adjusted to an OD_{600} of 0.1. Germination was monitored, and the number of germinated seeds was recorded at 2, 3, 4, and 7 dpi. The presence of *Neobacillus* sp. strain B4567 had no significant effect on either the germination kinetics or the final germination percentage compared with mock (Fig. S6A). However, measurement of primary root length at the end of the experiment revealed that seedlings grown in the presence of the bacteria developed significantly longer primary roots than control seedlings (Fig. S6B). These results indicate that strain B4567 did not affect tomato seed germination but promoted early root growth after germination.

Based on the ability of strain B4567 to promote root growth and tolerate moderately to high levels of osmotic and salinity stress, the strain was evaluated for its potential to improve tomato plant growth and yield under control and abiotic stress conditions. Tomato plants were grown in soil under normal irrigation, drought (30% soil water content), and moderate salinity (50 mM NaCl) conditions, with or without B4567 inoculation, and key growth and yield parameters were assessed (Fig. 8).

Inoculation with strain B4567 promoted tomato plant growth, as indicated by significant increases in stem diameter (Fig. 8B) and canopy diameter (Fig. 8C) under all tested conditions. In addition, bacterial inoculation significantly increased the dry weight of the aerial parts under control and salt stress conditions (Fig. 8D). Although plant height was also greater in inoculated plants under all tested conditions, these differences did not reach statistical significance (Fig. 8A).

Inoculation with strain B4567 also generally reduced the time to flowering (Fig. 8E) and fruit ripening (Fig. 8F) under the tested conditions. Regarding yield-related parameters, B4567 inoculation significantly increased both fruit number (Fig. 8G) and total fruit weight (Fig. 8H), while individual fruit weight was not significantly affected (Fig. 8I). We also measured the photosynthetic efficiency (F_v/F_m value) of tomato leaves under control and stress conditions. Although both stress treatments clearly reduced photosynthetic efficiency, no significant differences were observed between the mock- and B4567-inoculated plants (Fig. S7). These results suggest that the growth-promoting effect of bacterial inoculation is not associated with an increase in photosynthetic efficiency under the conditions tested.

To assess the overall effects of strain B4567 under abiotic stress, all measured parameters in drought- and salt-stressed plants were compared with those of the mock-inoculated, non-stressed control plants. The responses of drought-stressed mock-inoculated plants, drought-stressed B4567-inoculated plants, salt-stressed mock-inoculated plants, and salt-stressed B4567-inoculated plants were visualized as a heat map (Fig. 8J). Under drought stress, B4567 inoculation improved most of the measured parameters relative to the mock-inoculated, non-stressed controls. Dry weight and fruit ripening time, however, did not differ significantly from control levels. Although inoculation was associated with a reduction in individual fruit weight under drought stress, it increased fruit number and, consequently, total fruit weight. The heat map further indicated that salinity stress had a stronger overall effect on the measured parameters than drought stress. Nevertheless, inoculation with strain B4567 improved all assessed parameters under salinity stress, with canopy diameter and fruit number reaching levels that were not significantly different from those of the corresponding mock-inoculated, non-stressed control plants.

Discussion

In this study, we isolated and characterized *Neobacillus* sp. strain B4567, an endophytic bacterium recovered from *M. truncatula* grown under non-symbiotic greenhouse conditions. Screening of root-derived bacterial communities identified B4567 as a plant growth-promoting isolate with activity in several host species. Genome-based taxonomic analyses further indicated that it represents a distinct species within the genus *Neobacillus*. Functional characterization revealed the production of auxin-related compounds, tolerance to osmotic and saline stress, and biofilm formation under selected stress conditions. Importantly, inoculation promoted root development and increased tomato biomass and fruit yield under both control

and abiotic stress conditions. These findings highlight the potential of B4567 as a multifunctional plant growth-promoting bacterium.

Isolation and genomic characterization of *Neobacillus* sp. B4567

Legume roots harbor diverse microbial communities that constitute an important component of the plant microbiome (Hartman et al. 2017). Studies using *M. truncatula* as a model host have shown that soil origin and host genotype contribute to the organization of distinct microbial niches (Brown et al. 2020). In this context, the isolation of B4567 from surface-sterilized *M. truncatula* roots indicates its association with the internal root environment under the greenhouse conditions examined. Our screening strategy, which combined the isolation of root-associated bacterial communities with functional testing of individual isolates, enabled the identification of a bacterium with a reproducible growth-promoting effect. Notably, only one of the six isolates recovered from the beneficial bacterial mixture significantly promoted plant growth when tested individually, highlighting the importance of functional screening in identifying candidate PGPR.

Whole-genome sequencing and comparative phylogenomic analyses placed B4567 within the genus *Neobacillus*, which was established following the phylogenomic reclassification of the historically polyphyletic *Bacillus* group (Gupta et al. 2020; Patel and Gupta 2020). Although ribosomal multilocus sequence typing identified *N. drentensis* as its closest relative, the ANI and dDDH values obtained in comparisons with *N. drentensis* and *N. nitrireducens* were substantially below the accepted species delineation thresholds. These results support the classification of B4567 as a distinct, previously undescribed species within the genus *Neobacillus*.

The genome size and coding capacity of B4567 fall within the range reported for plant-growth-promoting *Bacillus* species and related taxa, which typically possess genomes of 4.5–7.5 Mbp encoding 4,402–6,697 proteins (Cangioli et al. 2024). Similar genomic features have been reported for endophytic isolates such as *Bacillus* sp. EB-40 (Pereira et al. 2024). Of particular interest is the large megaplasmid of B4567, which carries genes associated with conjugation and replication, as well as genes potentially involved in sporulation, formaldehyde and reactive oxygen species (ROS) detoxification, and alternative nitrogen utilization. The chromosome also contains 15 copies of the rRNA operon, a feature previously associated with rapid growth and adaptation to changing environmental conditions (Klappenbach et al. 2000).

Such genomic characteristics may be advantageous in dynamic root-associated environments, although their contribution to the observed growth-promoting activity and stress tolerance of B4567 remains to be established.

Genome-based pathogenicity prediction indicated a low probability of pathogenicity, consistent with the absence of reported pathogenicity-associated features in other beneficial bacterial strains considered for biofertilizer applications (Cangioli et al. 2024). This result is encouraging for the potential development of B4567 as a bioinoculant, although dedicated biosafety assessments will be required.

Broad-host plant growth promotion and preferential stimulation of root development

B4567 promoted plant growth in several taxonomically diverse species, including the dicotyledonous plants *M. truncatula*, *S. lycopersicum*, and *N. benthamiana*, as well as the monocotyledonous species *B. distachyon*. The increased root and shoot biomass in these hosts suggests that its growth-promoting activity is not restricted to its original host species. Although further testing is needed to establish the full host range, these findings indicate considerable potential for application across different plant species.

Time-course analysis in tomato revealed that the growth response was initially more pronounced in roots than in shoots. Root biomass increased significantly as early as four days after inoculation, whereas differences in shoot biomass became apparent only at later time points. This temporal pattern suggests that root development is an early target of B4567-mediated growth promotion and may contribute to the subsequent increase in shoot biomass. Consistent with this interpretation, inoculated plants developed significantly more secondary lateral roots, while primary lateral root numbers remained comparable to those of mock-inoculated controls.

The preferential stimulation of higher-order lateral roots suggests that B4567 modifies specific parts of root system architecture rather than promoting all components of root development. Increased lateral root growth is a well-established response to PGPR inoculation and can enhance roots to absorb more water and nutrients (Vacheron et al. 2013). The fact that the number of primary lateral roots did not change much might be because the first primary lateral root primordia had already started forming and were beginning to grow out at the time of inoculation. In contrast, subsequent lateral root development may still have responded to the

bacteria, pointing to a future investigation, inoculating at different stages of plant growth to see how that affects root development.

The increase in secondary lateral roots is also consistent with the auxin dependence of lateral root initiation and development (Grover et al. 2021) and with previous evidence that bacterial auxin production can stimulate lateral root proliferation in a concentration-dependent manner (Patten and Glick 2002; Vacheron et al. 2013). Thus, the root architectural changes induced by B4567 may reflect alterations in auxin-dependent developmental processes. Beyond their effects on resource acquisition, changes in root architecture can also influence the composition and availability of root exudates, potentially affecting interactions with other rhizosphere microorganisms (Khoso et al. 2024). Whether B4567-induced root remodeling has such broader effects on the root-associated microbiome remains to be investigated.

Auxin-related compound production as a potential contributor to root growth promotion

Among the plant growth-promoting traits examined, B4567 did not show detectable inorganic phosphate solubilization, siderophore production, or ACC deaminase activity under the conditions tested. The absence of detectable ACC deaminase activity was consistent with the lack of an identifiable canonical *acsdS* gene in its genome. ACC deaminase is a well-characterized PGPR trait that can alleviate ethylene-mediated growth inhibition by degrading ACC, the immediate precursor of ethylene (Shahid et al. 2023; Ferreira et al. 2025). Its absence suggests that this mechanism is unlikely to contribute to the growth-promoting activity of B4567.

In contrast, B4567 produced substantial amounts of Salkowski-reactive compounds when cultivated in tryptophan-supplemented medium. The estimated concentrations, expressed as IAA equivalents, reached approximately 19.5 μg ml^{-1} after 24 h and 10.5 μg ml^{-1} after 48 h. No detectable compounds were observed in cultures grown without supplemental tryptophan, suggesting that their production depends on the availability of an external tryptophan source under the conditions tested. This is consistent with the involvement of tryptophan-dependent pathways in bacterial auxin biosynthesis. In agreement with this possibility, genome annotation identified genes potentially associated with IAA biosynthetic pathways involving tryptamine and indole-3-acetamide intermediates.

Microbially produced auxins can modify local auxin availability and signaling in plant roots. As a central regulator of root development, auxin influences lateral root initiation and emergence, while its effects on primary root elongation and lateral root formation depend on concentration, tissue context, and developmental stage (Overvoorde et al. 2010; Vacheron et al. 2013; Tsukanova et al. 2017; Qian and Bai 2021). Previous studies have shown that bacterial auxin production can stimulate lateral root and root hair development (Patten and Glick 2002; Vacheron et al. 2013). Accordingly, the production of auxin-related compounds by B4567 provides a plausible explanation for the increased root biomass and secondary lateral root proliferation observed in inoculated tomato plants.

However, a direct causal relationship between bacterial auxin production and the observed root architectural changes has not been established. The Salkowski assay detects several indolic compounds and cannot specifically distinguish IAA from other Salkowski-reactive metabolites (Guardado-Fierros et al. 2024). Therefore, the measured concentrations should be interpreted as IAA equivalents rather than definitive measurements of IAA. Targeted chemical analysis of bacterial culture supernatants and characterization of the putative biosynthetic pathways will be necessary to establish the identity of the compounds produced and their contribution to plant growth promotion.

Stress tolerance and biofilm formation as potentially beneficial bacterial traits

B4567 displayed considerable tolerance to osmotic and saline stress *in vitro*. Increasing PEG concentrations progressively inhibited bacterial growth, although the strain retained detectable growth at 20% PEG. At 30% PEG, no growth or viability was detected. In contrast, B4567 maintained viability and the capacity for growth at NaCl concentrations up to 15% (w/v), although increasing salinity prolonged the lag phase. These results indicate substantial bacterial stress tolerance, particularly under saline conditions.

The ability to withstand osmotic and saline stress may be advantageous for bacteria inhabiting root-associated environments, where water availability and ionic conditions fluctuate under drought and salinity (Gupta et al. 2022). However, PEG- and NaCl-based assays represent simplified *in vitro* conditions and do not fully reproduce the physicochemical complexity of soil. In particular, PEG-mediated osmotic stress does not encompass all aspects of soil drying, whereas NaCl imposes both osmotic and ion-specific effects. Consequently, the observed stress

tolerance indicates the potential environmental resilience of B4567 but does not directly demonstrate its persistence or activity in stressed soil.

B4567 also formed biofilms under control conditions and retained this capacity under selected stress conditions. Biofilm formation was maintained in the presence of 20% PEG, despite the substantial reduction in bacterial growth, whereas under saline conditions it was detected at 5% NaCl but was strongly reduced or absent at higher concentrations. Such differences in biofilm responses to salinity have been reported among PGPR strains. For example, salt exposure increased biofilm formation in some isolates (Kasim et al. 2016), whereas substantial reductions were observed in others, including *Bacillus amyloliquefaciens* GB03 (Cappellari et al. 2023). High salinity can affect biofilm stability by altering the properties of exopolysaccharides, which contribute to biofilm structure (Kumar et al. 2020). The reduced biofilm formation observed at higher NaCl concentrations in B4567 may therefore reflect the sensitivity of its biofilm matrix to saline conditions.

Biofilms can facilitate bacterial attachment to surfaces and contribute to persistence in root-associated environments. In addition, the production of exopolysaccharides and other stress-protective compounds by PGPR can support plant growth under saline conditions (Shultana et al. 2022). The ROS-detoxification genes identified on the B4567 megaplasmid may also contribute to bacterial stress responses, although their expression and functional significance remain unknown. Overall, the combination of osmotic and saline stress tolerance with biofilm-forming capacity suggests that B4567 possesses traits potentially favorable for persistence under variable environmental conditions. Direct assessment of root colonization and survival in stressed soil will be necessary to determine the contribution of these traits to plant growth-promoting activity of B4567.

Effects of B4567 on tomato growth and productivity under drought and salinity stress

The growth-promoting effects of B4567 under controlled conditions prompted us to investigate its potential to improve tomato performance in soil under drought and salinity stress. Inoculation did not significantly affect seed germination or germination kinetics but resulted in longer primary roots in young seedlings. This indicates that B4567 promotes early post-germination root growth rather than the germination process itself, consistent with the root-biased growth response observed in established plants.

In soil-based experiments, B4567 increased stem and canopy diameter under control, drought, and salinity conditions. Shoot dry weight was also significantly increased under control and salinity conditions, whereas plant height showed a consistent but nonsignificant increase. These findings indicate that the growth-promoting effects of B4567 extend in different water and salinity regimes.

The effects on reproductive development and yield were particularly notable. Inoculation generally accelerated flowering and fruit ripening and significantly increased fruit number and total fruit weight, whereas individual fruit weight was not significantly affected overall. Thus, the increase in total yield was primarily associated with a greater number of fruits rather than increased individual fruit size. Under drought stress, individual fruit weight was reduced, but the increase in fruit number resulted in higher total fruit weight. This suggests that B4567 can improve reproductive output even when individual fruit development remains constrained by water limitation.

The beneficial effects of B4567 are consistent with previous reports of PGPR-mediated improvements in plant performance under salinity and drought. For example, salt-stress-mitigating bacterial strains have been shown to increase plant biomass under saline conditions (Cappellari et al. 2023), while biofilm-forming PGPR can alleviate salinity-associated reductions in seedling growth and relative water content (Kasim et al. 2016). Similarly, field experiments have demonstrated increased maize yield following inoculation with *Pseudomonas putida* under drought conditions (Kálmán et al. 2024). Together, these findings support the potential of beneficial bacteria to improve crop performance under abiotic stress, although the magnitude and nature of the response depend on the bacterial strain, host plant, and environmental conditions.

The heat-map analysis indicated that salinity had a stronger overall effect on the measured plant traits than drought under the conditions examined. Nevertheless, B4567 inoculation improved several growth and yield parameters under salinity stress. Canopy diameter and fruit number in salt-stressed inoculated plants were not significantly different from those of mock-inoculated, non-stressed controls. This suggests that inoculation partially compensated for the negative effects of salinity on tomato development and reproductive performance. Under drought stress, inoculation also improved most measured parameters relative to the non-stressed mock control, although some traits, including dry weight and fruit ripening time, remained affected.

Despite these improvements in growth and yield, B4567 inoculation did not significantly affect leaf photosynthetic efficiency, as measured by the F_v/F_m ratio, under either control or stress conditions. Thus, the growth-promoting effects cannot be attributed to a detectable improvement in maximum photosystem II efficiency. Other processes, including changes in root development, resource acquisition, or plant water and nutrient relations, may contribute to the observed responses. However, these possibilities remain to be tested.

Overall, the soil-based experiments demonstrate that B4567 improves several aspects of tomato growth and productivity under both control and abiotic stress conditions. The increase in total fruit yield is particularly relevant from an agricultural perspective, as it demonstrates that the beneficial effects of inoculation extend beyond vegetative growth. Further evaluation across soil types, stress intensities, and cultivation systems will be necessary to establish the consistency and practical applicability of these effects.

Acknowledgments

This work was supported by the National Research, Development and Innovation Office (NRDI Office Research Grant no. K150440 and 2021-1.2.6-TÉT-IPARI-MA-2022-00005 to PK and PD146655 to SK) and by HUN-REN BRC (454004 to PK). PK and ÁD were supported by the Flagship Research Groups Programme and by the Research Excellence Programme (2024) of the Hungarian University of Agriculture and Life Sciences. This project contributes to the activities of the COST Action “ROOT-BENEFIT” (CA22142) and “BIORAG” (CA25180), supported by the European Cooperation in Science and Technology (COST). We thank Sándor Jenei for his skillful technical assistance and László Szilák for his scientific support.

Author contributions SK, LS, GM and PK conceived and designed the project. SK, ÁD, GD, BT, DD, and BU performed the experiments and evaluated the results. AK and PG analyzed sequence data. SK, PG and PK wrote and edited the manuscript.

Data Availability Statement

The assembled genome and raw sequencing data were deposited in the GenBank and SRA databases, respectively, under the NCBI BioProject number PRJNA1516868.

Statements and Declarations

Conflict of Interest

The authors declare no conflict of interest.

Supplementary Information

The online version contains supplementary material available at (link)

Fig. S1. Colony morphology of bacterial isolates obtained from *Medicago truncatula* root tissues.

Fig. S2. Time-course analysis of the growth-promoting effect of the *Neobacillus* sp. strain B4567.

Fig. S3. Root biomass and architecture of tomato plants grown in a rhizotron system.

Fig. S4. Biofilm formation by *Neobacillus* sp. strain B4567.

Fig. S5. Indole-3-acetic acid (IAA) biosynthesis pathways in the genome of *Neobacillus* sp. strain B4567.

Fig. S6. Effect of *Neobacillus* sp. strain B4567 on tomato seed germination and primary root growth.

Fig. S7. Effect of bacterial treatment on photosynthetic performance.

References

Barker DG, Pfaff T, Moreau D, et al (2006) Growing *M. truncatula*: choice of substrates and growth conditions. In: Mathesius U, Journet E-P (eds) Medicago truncatula handbook. The Samuel Roberts Noble Foundation, Ardmore, USA, pp 1–26

Bhattacharjee K, Barua S, Chrungoo NK, Joshi SR (2023) Characterization of Biomineralizing and Plant Growth-Promoting Attributes of Lithobiontic Bacteria. Curr Microbiol 80:80. https://doi.org/10.1007/s00284-022-03176-x

Brown SP, Grillo MA, Podowski JC, Heath KD (2020) Soil origin and plant genotype structure distinct microbiome compartments in the model legume Medicago truncatula. Microbiome 8:139. https://doi.org/10.1186/s40168-020-00915-9

Cangioli L, Tabacchioni S, Visca A, et al (2024) Genome Insights into Beneficial Microbial Strains Composing SIMBA Microbial Consortia Applied as Biofertilizers for Maize,

Wheat and Tomato. Microorganisms 12:2562. https://doi.org/10.3390/microorganisms12122562

Cappellari LDR, Bogino PC, Nievas F, et al (2023) Exploring the Differential Impact of Salt Stress on Root Colonization Adaptation Mechanisms in Plant Growth-Promoting Rhizobacteria. Plants 12:4059. https://doi.org/10.3390/plants12234059

Chen S, Zhou Y, Chen Y, Gu J (2018) fastp: an ultra-fast all-in-one FASTQ preprocessor. Bioinformatics 34:i884–i890. https://doi.org/10.1093/bioinformatics/bty560

Chklovski A, Parks DH, Woodcroft BJ, Tyson GW (2023) CheckM2: a rapid, scalable and accurate tool for assessing microbial genome quality using machine learning. Nat Methods 20:1203–1212. https://doi.org/10.1038/s41592-023-01940-w

Dworkin M, Foster JW (1958) Experiments with some microorganisms which utilize ethane and hydrogen. J Bacteriol 75:592–603. https://doi.org/10.1128/jb.75.5.592-603.1958

Edgar RC (2004) MUSCLE: multiple sequence alignment with high accuracy and high throughput. Nucleic Acids Res 32:1792–1797. https://doi.org/10.1093/nar/gkh340

Ferreira JP, Vidal MS, Baldani JI (2025) Exploring ACC deaminase-producing bacteria for drought stress mitigation in Brachiaria. Front Plant Sci 16:1607697. https://doi.org/10.3389/fpls.2025.1607697

Garvin DF, Gu Y, Hasterok R, et al (2008) Development of Genetic and Genomic Research Resources for *Brachypodium distachyon*, a New Model System for Grass Crop Research. Crop Sci 48:. https://doi.org/10.2135/cropsci2007.06.0332tpg

Giehl RFH, Gruber BD, von Wirén N (2014) It's time to make changes: modulation of root system architecture by nutrient signals. J Exp Bot 65:769–778. https://doi.org/10.1093/jxb/ert421

Goris J, Konstantinidis KT, Klappenbach JA, et al (2007) DNA–DNA hybridization values and their relationship to whole-genome sequence similarities. Int J Syst Evol Microbiol 57:81–91. https://doi.org/10.1099/ijs.0.64483-0

Grover M, Bodhankar S, Sharma A, et al (2021) PGPR Mediated Alterations in Root Traits: Way Toward Sustainable Crop Production. Front Sustain Food Syst 4:618230. https://doi.org/10.3389/fsufs.2020.618230

Guardado-Fierros BG, Tuesta-Popolizio DA, Lorenzo-Santiago MA, et al (2024) Comparative study between Salkowski reagent and chromatographic method for auxins quantification from bacterial production. Front Plant Sci 15:. https://doi.org/10.3389/fpls.2024.1378079

Gupta A, Mishra R, Rai S, et al (2022) Mechanistic Insights of Plant Growth Promoting Bacteria Mediated Drought and Salt Stress Tolerance in Plants for Sustainable Agriculture. Int J Mol Sci 23:3741. https://doi.org/10.3390/ijms23073741

Gupta RS, Patel S, Saini N, Chen S (2020) Robust demarcation of 17 distinct Bacillus species clades, proposed as novel Bacillaceae genera, by phylogenomics and comparative genomic analyses: description of Robertmurraya kyonggiensis sp. nov. and proposal for

an emended genus Bacillus limiting it only to the members of the Subtilis and Cereus clades of species. Int J Syst Evol Microbiol 70:5753–5798. https://doi.org/10.1099/ijsem.0.004475

Han DM, Choi DG, Baek JH, et al (2023) Neobacillus terrae sp. nov., isolated from mountain soil. Int J Syst Evol Microbiol 73:. https://doi.org/10.1099/ijsem.0.005818

Hartman K, Van Der Heijden MG, Roussely-Provent V, et al (2017) Deciphering composition and function of the root microbiome of a legume plant. Microbiome 5:2. https://doi.org/10.1186/s40168-016-0220-z

He S, Li L, Lv M, et al (2024) PGPR: Key to Enhancing Crop Productivity and Achieving Sustainable Agriculture. Curr Microbiol 81:377. https://doi.org/10.1007/s00284-024-03893-5

Hernández-Plaza A, Deng Z, Robledo-Yagüe F, et al (2026) eggNOG v7: phylogeny-based orthology predictions and functional annotations. Nucleic Acids Res 54:D402–D408. https://doi.org/10.1093/nar/gkaf1249

Irfan MF, Shafique S, Shafique S, et al (2026) Molecular pathways in plant growth-promoting rhizobacteria–plant interactions: a comprehensive review. Arch Microbiol 208:205. https://doi.org/10.1007/s00203-026-04749-1

Jochum MD, McWilliams KL, Borrego EJ, et al (2019) Bioprospecting Plant Growth-Promoting Rhizobacteria That Mitigate Drought Stress in Grasses. Front Microbiol 10:2106. https://doi.org/10.3389/fmicb.2019.02106

Jolley KA, Bray JE, Maiden MCJ (2018) Open-access bacterial population genomics: BIGSdb software, the PubMLST.org website and their applications. Wellcome Open Res 3:124. https://doi.org/10.12688/wellcomeopenres.14826.1

Kálmán CD, Nagy Z, Berényi A, et al (2024) Investigating PGPR bacteria for their competence to protect hybrid maize from the factor drought stress. Cereal Res Commun 52:129–150. https://doi.org/10.1007/s42976-023-00388-0

Kämpfer P, Glaeser SP, McInroy JA, et al (2022) Neobacillus rhizosphaerae sp. nov., isolated from the rhizosphere, and reclassification of Bacillus dielmonensis as Neobacillus dielmonensis comb. nov. Int J Syst Evol Microbiol 72:005636. https://doi.org/10.1099/ijsem.0.005636

Kanehisa M, Sato Y, Kawashima M (2022) KEGG mapping tools for uncovering hidden features in biological data. Protein Sci 31:47–53. https://doi.org/10.1002/pro.4172

Kasim WA, Gaafar RM, Abou-Ali RM, et al (2016) Effect of biofilm forming plant growth promoting rhizobacteria on salinity tolerance in barley. Ann Agric Sci 61:217–227. https://doi.org/10.1016/j.aoas.2016.07.003

Khoso MA, Wagan S, Alam I, et al (2024) Impact of plant growth-promoting rhizobacteria (PGPR) on plant nutrition and root characteristics: Current perspective. Plant Stress 11:100341. https://doi.org/10.1016/j.stress.2023.100341

Klappenbach JA, Dunbar JM, Schmidt TM (2000) rRNA Operon Copy Number Reflects Ecological Strategies of Bacteria. Appl Environ Microbiol 66:1328–1333. https://doi.org/10.1128/AEM.66.4.1328-1333.2000

Kloepper JW (1978) Plant growth-promoting rhizobacteria on radishes. In: Proc. of the 4th Internet. Conf. on Plant Pathogenic Bacter, Station de Pathologie Vegetale et Phytobacteriologie, INRA, Angers, France, 1978. pp 879–882

Kumar A, Singh S, Gaurav AK, et al (2020) Plant Growth-Promoting Bacteria: Biological Tools for the Mitigation of Salinity Stress in Plants. Front Microbiol 11:1216. https://doi.org/10.3389/fmicb.2020.01216

Lugtenberg B, Kamilova F (2009) Plant-Growth-Promoting Rhizobacteria. Annu Rev Microbiol 63:541–556. https://doi.org/10.1146/annurev.micro.62.081307.162918

Mann S, Chen Y-PP (2010) Bacterial genomic G + C composition-eliciting environmental adaptation. Genomics 95:7–15. https://doi.org/10.1016/j.ygeno.2009.09.002

Martínez-Hidalgo P, Flores-Félix JD, Sánchez-Juanes F, et al (2021) Identification of Canola Roots Endophytic Bacteria and Analysis of Their Potential as Biofertilizers for Canola Crops with Special Emphasis on Sporulating Bacteria. Agronomy 11:1796. https://doi.org/10.3390/agronomy11091796

Meier-Kolthoff JP, Carbasse JS, Peinado-Olarte RL, Göker M (2022) TYGS and LPSN: a database tandem for fast and reliable genome-based classification and nomenclature of prokaryotes. Nucleic Acids Res 50:D801–D807. https://doi.org/10.1093/nar/gkab902

Meier-Kolthoff JP, Klenk H-P, Göker M (2014) Taxonomic use of DNA G+C content and DNA–DNA hybridization in the genomic age. Int J Syst Evol Microbiol 64:352–356. https://doi.org/10.1099/ijs.0.056994-0

Moharana A, Dhruw L, Chakraborty A, et al (2026) Rhizobacteria-Mediated Reprogramming of Phytohormone Landscapes for Mitigating Salinity Stress in Plants. Int J Mol Sci 27:7494. https://doi.org/10.3390/ijms27167494

Overvoorde P, Fukaki H, Beeckman T (2010) Auxin Control of Root Development. Cold Spring Harb Perspect Biol 2:a001537. https://doi.org/10.1101/cshperspect.a001537

Patel S, Gupta RS (2020) A phylogenomic and comparative genomic framework for resolving the polyphyly of the genus Bacillus: Proposal for six new genera of Bacillus species, Peribacillus gen. nov., Cytobacillus gen. nov., Mesobacillus gen. nov., Neobacillus gen. nov., Metabacillus gen. nov. and Alkalihalobacillus gen. nov. Int J Syst Evol Microbiol 70:406–438. https://doi.org/10.1099/ijsem.0.003775

Patten CL, Glick BR (2002) Role of *Pseudomonas putida* Indoleacetic Acid in Development of the Host Plant Root System. Appl Environ Microbiol 68:3795–3801. https://doi.org/10.1128/AEM.68.8.3795-3801.2002

Pattison RJ, Csukasi F, Catalá C (2014) Mechanisms regulating auxin action during fruit development. Physiol Plant 151:62–72. https://doi.org/10.1111/ppl.12142

Pereira FGS, Vidigal PMP, Santos SA, et al (2024) Genome sequencing of Bacillus sp. isolate EB-40: a plant growth-promoting bacteria

Pikovskaya RI (1948) Mobilization of phosphorus in soil in connection with the vital activity of some microbial species. Mikrobiologiya 17:362–370

Qian J-M, Bai Y (2021) Stuck on you: Bacterial-auxin-mediated bacterial colonization of plant roots. Cell Host Microbe 29:1471–1473. https://doi.org/10.1016/j.chom.2021.09.014

Richter M, Rosselló-Móra R, Oliver Glöckner F, Peplies J (2016) JSpeciesWS: a web server for prokaryotic species circumscription based on pairwise genome comparison. Bioinformatics 32:929–931. https://doi.org/10.1093/bioinformatics/btv681

Rosier A, Medeiros FHV, Bais HP (2018) Defining plant growth promoting rhizobacteria molecular and biochemical networks in beneficial plant-microbe interactions. Plant Soil 428:35–55. https://doi.org/10.1007/s11104-018-3679-5

Ryu C-M, Nelson LM, de-Bashan L (2024) Editorial: Highlights from the 12th plant growth-promoting rhizobacteria workshop. Front Plant Sci 15:1470576. https://doi.org/10.3389/fpls.2024.1470576

Salkowski E (1885) Ueber das Verhalten der Skatolcarbonsäure im Organismus. bchm 9:23–33. https://doi.org/10.1515/bchm1.1885.9.1.23

Shahid M, Singh UB, Khan MS, et al (2023) Bacterial ACC deaminase: Insights into enzymology, biochemistry, genetics, and potential role in amelioration of environmental stress in crop plants. Front Microbiol 14:. https://doi.org/10.3389/fmicb.2023.1132770

Shahwar D, Mushtaq Z, Mushtaq H, et al (2023) Role of microbial inoculants as bio fertilizers for improving crop productivity: A review. Heliyon 9:. https://doi.org/10.1016/j.heliyon.2023.e16134

Shultana R, Zuan ATK, Naher UA, et al (2022) The PGPR Mechanisms of Salt Stress Adaptation and Plant Growth Promotion. Agronomy 12:2266. https://doi.org/10.3390/agronomy12102266

Tamura K, Stecher G, Kumar S (2021) MEGA11: Molecular Evolutionary Genetics Analysis Version 11. Mol Biol Evol 38:3022–3027. https://doi.org/10.1093/molbev/msab120

Tatusova T, DiCuccio M, Badretdin A, et al (2016) NCBI prokaryotic genome annotation pipeline. Nucleic Acids Res 44:6614–6624. https://doi.org/10.1093/nar/gkw569

Tegenfeldt F, Kuznetsov D, Manni M, et al (2025) OrthoDB and BUSCO update: annotation of orthologs with wider sampling of genomes. Nucleic Acids Res 53:D516–D522. https://doi.org/10.1093/nar/gkae987

Tsukanova KA, Chebotar VK, Meyer JJM, Bibikova TN (2017) Effect of plant growth-promoting Rhizobacteria on plant hormone homeostasis. South Afr J Bot 113:91–102. https://doi.org/10.1016/j.sajb.2017.07.007

941 Vacheron J, Desbrosses G, Bouffaud M-L, et al (2013) Plant growth-promoting rhizobacteria
942 and root system functioning. Front Plant Sci 4:. https://doi.org/10.3389/fpls.2013.00356

943 Wick RR, Holt KE (2022) Polypolish: Short-read polishing of long-read bacterial genome
944 assemblies. PLOS Comput Biol 18:e1009802.
945 https://doi.org/10.1371/journal.pcbi.1009802

946 Wick RR, Judd LM, Cerdeira LT, et al (2021) Trycycler: consensus long-read assemblies for
947 bacterial genomes. Genome Biol 22:266. https://doi.org/10.1186/s13059-021-02483-z

948 Yang J, Kloepper JW, Ryu C-M (2009) Rhizosphere bacteria help plants tolerate abiotic stress.
949 Trends Plant Sci 14:1–4. https://doi.org/10.1016/j.tplants.2008.10.004

950 Zerrouk IZ, Benchabane M, Khelifi L, et al (2016) A *Pseudomonas* strain isolated from date-
951 palm rhizospheres improves root growth and promotes root formation in maize exposed
952 to salt and aluminum stress. J Plant Physiol 191:111–119.
953 https://doi.org/10.1016/j.jplph.2015.12.009

954 Zhao X, Yuan X, Xing Y, et al (2023) A meta-analysis on morphological, physiological and
955 biochemical responses of plants with PGPR inoculation under drought stress. Plant Cell
956 Environ 46:199–214. https://doi.org/10.1111/pce.14466

957 Zhao Y (2018) Essential Roles of Local Auxin Biosynthesis in Plant Development and in
958 Adaptation to Environmental Changes. Annu Rev Plant Biol 69:417–435.
959 https://doi.org/10.1146/annurev-arplant-042817-040226

960

961

962

963 **Figure legends**

964 **Fig. 1** Identification of a novel plant growth-promoting rhizobacterium (PGPR) isolated from
965 *Medicago truncatula* roots. Representative images of a mock-inoculated *M. truncatula* plant
966 (A), plant inoculated with the bacterial mixture designated “9” (B), and a plant inoculated with
967 the purified single bacterial isolate “9.6” (C), four weeks post-inoculation. Root (D) and shoot
968 (E) dry weights of plants inoculated with mixture “9” or with individual bacterial isolates
969 recovered from the roots of plants inoculated with mixture “9” are shown in comparison with
970 those of mock-inoculated control plants. Statistical significance was assessed using unpaired *t*-
971 tests. n=8 plants per treatment. Scale bar: 7 mm

Fig. 2 Phylogenetic relationship of *Neobacillus* sp. strain B4567 with related bacteria. (A) The least divergent sequence (locus tag: AC7SJ9_00150) of the 15 copies of the 16S rRNA gene sequences from the *Neobacillus* sp. strain B4567 genome and of the representative members of selected genera within the family *Bacillaceae* were retrieved and used for phylogenetic analysis. *Staphylococcus aureus* strain ATCC 12600, a member of the family *Staphylococcaceae*, was included as the outgroup. The phylogenetic tree was constructed using the Maximum Likelihood method based on the General Time Reversible model with gamma-distributed rate variation and invariant sites (GTR+G+I). Branch lengths represent the number of substitutions per site. Bootstrap support values, calculated from 1,000 replicates, are shown adjacent to the corresponding branches. A total of 1,465 nucleotide positions were included in the final dataset. (B) Phylogenetic relationship of *Neobacillus* sp. strain B4567 with other members of the genus *Neobacillus* based on whole-genome sequences. The minimum-evolution phylogenetic tree was constructed by the Type Strain Genome Server (TYGS) using Genome BLAST Distance Phylogeny (GBDP) distances derived from whole-genome sequences. Branch lengths are scaled according to the GBDP distance formula *d5*. Numbers adjacent to the branches represent pseudo-bootstrap support values based on 100 replicates. The GenBank identifiers are included for all sequences.

Fig. 3 The *Neobacillus* sp. strain B4567 promotes growth of *Solanum lycopersicum*, *Brachypodium distachyon*, and *Nicotiana benthamiana* species. Representative images of mock-inoculated control plants (left) and plants inoculated with *Neobacillus* sp**.** strain B4567 (right) are shown for *S. lycopersicum* (A), *B. distachyon* (B), and *N. benthamiana* (C). Dry weights of shoot and root tissues were measured four weeks post-inoculation for *S. lycopersicum* (D), *B. distachyon* (E), and *N. benthamiana* (F), and compared with mock-inoculated controls. Statistical significance between treatments was assessed using unpaired $t-$ tests. Significance levels are indicated as *** ($p \leq 0.001$). Sample size: n = 20–24 plants across three biological replicates

Fig. 4 Time-course analysis of root and shoot biomass following inoculation with *Neobacillus* sp. strain B4567. Dry weights of root (A) and shoot (B) tissues were measured at multiple time points to assess growth kinetics in B4567-inoculated and mock-inoculated plants. Early time points (4, 7, and 10 dpi), highlighted by red boxes, revealed a significant increase in root biomass in inoculated plants, while shoot biomass remained comparable to mock-inoculated controls. Statistical significance was assessed using unpaired *t*-tests. Significance levels are

indicated as follows: ns, $p > 0.05$; *, $p \leq 0.05$; **, $p \leq 0.01$; ***. $p \leq 0.001$. Sample size: n = 15–27 plants per time points across three biological replicates

Fig. 5 Inoculation with *Neobacillus* sp. strain B4567 promotes lateral root formation and root branching in tomato plants. Quantification of primary and secondary lateral roots in inoculated (B4567) and mock-inoculated tomato plants at 14 dpi. Statistical significance was assessed using unpaired *t*-tests. Significance levels are indicated as follows: ns, $p > 0.05$; ***, $p \leq 0.001$. Scale bar = 7 mm. Sample size: n = 21 plants per treatment across three biological replicates

Fig. 6 Production of auxin-related compounds by *Neobacillus* sp. strain B4567. (A) Bacterial growth was monitored by measuring OD_{600} after 24 and 48 h of incubation in mock liquid YMA medium (YMA) or tryptophan-supplemented liquid YMA medium (YMA+Trp). (B) Auxin-related compound production was assessed using the Salkowski assay by measuring absorbance at OD_{530} in cell-free supernatants collected after 24 and 48 h of incubation. (C) Concentrations of auxin-related compounds in cell-free supernatants from the tryptophan-supplemented cultures were estimated using a calibration curve generated with IAA standards. n = 5 biological replicates with 3 technical replicates

Fig. 7 Stress tolerance and biofilm formation of *Neobacillus* sp. strain B4567 strain under osmotic and salinity stress conditions. Kinetic growth curves of *Neobacillus* sp. strain B4567 were monitored in TY control medium and in media supplemented with 10%, 20%, and 30% (w/v) polyethylene glycol (PEG) to impose osmotic stress (A), or with 5%, 10%, and 15% (w/v) NaCl to impose salinity stress (C). Cell viability was evaluated by spot assays on TY agar plates using cultures grown under the corresponding conditions for 72 hours of incubation (B). Biofilm formation under normal and stress conditions was quantified after 6 days of incubation in the respective medium (D). For the growth curve analysis, n = 11 biological replicates per condition; for the spot assay, n = 4 biological replicates per condition; and for biofilm quantification, n = 3 biological replicates per condition

Fig. 8 Application of *Neobacillus* sp. strain B4567 promotes tomato growth and yield under control, drought, and salinity stress conditions. (A–I) Vegetative traits, including plant height, stem diameter, canopy diameter, and shoot dry weight, and reproductive traits, including time to flowering, fruit ripening time, fruit number, total fruit weight and individual fruit weight, were measured in tomato plants grown under control, drought and salinity stress conditions and compared with mock controls. (J) Heat map showing the effects of bacterial inoculation on plant responses to drought and salinity stress. Heatmap showing adjusted *p*-values obtained

from Dunnett's post-hoc test following one-way ANOVA for each evaluated trait. Comparisons were performed across experimental conditions with the Control mock sample set as the reference group. The color gradient represents the level of statistical significance (adjusted *p*-value), with non-significant differences ($p \geq 0.05$) explicitly denoted as 'ns'. The Control condition was excluded from the visualization to highlight stress-related treatment comparisons. n = 12–17 plants across two to three biological replicates

Table 1. Summary of PGP tests conducted to characterize the novel *Neobacillus* sp. strain B4567.

Supplementary figure legends

Fig. S1. Colony morphology of bacterial isolates obtained from *Medicago truncatula* root tissues. Colony morphology of isolates 9.1–9.5 (A–E) and the novel plant growth-promoting rhizobacterial isolate 9.6, *Neobacillus* sp. strain B4567 (F).

Fig. S2. Time-course analysis of the growth-promoting effect of the *Neobacillus* sp. strain B4567 on tomato plants. Representative images of control plants (A, C, E, G) and plants inoculated with *Neobacillus* sp. strain B4567 (B, D, F, H) plants at 0, 4, 10, and 18 days post-inoculation (dpi).

Fig. S3. Root biomass and architecture of tomato plants grown in a rhizotron system four weeks post-inoculation with the *Neobacillus* sp. strain B4567**.** Representative images of non-inoculated control plants (A) and plants inoculated with the *Neobacillus* sp. strain B4567 (B). The rhizotron system enabled visualization of root system size, branching pattern, and overall structural development.

Fig. S4. Biofilm formation by *Neobacillus* sp. strain B4567 under normal and stress conditions**.** Representative images of biofilm formation by *Neobacillus* sp. strain B4567 after 4 (A) and 6 (B) days of incubation in TY medium. Biofilm development was additionally assessed after 6 days of incubation in TY medium supplemented with various concentrations of polyethylene glycol (PEG-6000) (C) or NaCl (D) to impose osmotic and salinity stress, respectively.

Fig. S5. Presence of indole-3-acetic acid (IAA) biosynthesis pathways in the genome of *Neobacillus* sp. strain B4567. Pathway components were identified by assigning KEGG Orthology (KO) numbers to the predicted proteins of strain B4567 using the eggNOG Mapper v3 server, followed by mapping the assigned KO numbers onto the predefined metabolic

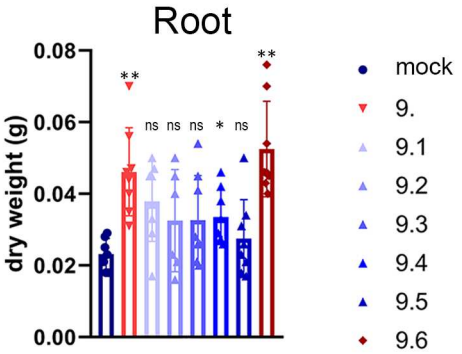
pathways by the KEGG Mapper Reconstruct tool. The potentially existing functions are highlighted in green on the metabolic pathway map.

Fig. S6. Effect of *Neobacillus* sp. strain B4567 on tomato seed germination and primary root growth. Germination kinetics (A) and primary root length (radicle length) (B) of tomato seedlings grown on half-strength Murashige and Skoog (½ MS) medium without bacterial inoculation (Mock) or supplemented with a bacterial suspension adjusted to an OD_{600} of 0.1 (B4567). No significant differences were observed in germination kinetics or final germination percentage. In contrast, seedlings grown in the presence of strain B4567 developed significantly longer primary roots than control seedlings. Statistical significance was assessed using unpaired *t*-tests. Significance levels: ns, $p \geq 0.05$; *, $p < 0.05$. For the analysis of germination kinetics, 100 seeds per treatment were analyzed across four biological replicates. Primary root length was measured in 88 control seedlings grown on ½ MS medium and 89 seedlings grown on ½ MS medium supplemented with *Neobacillus* sp. strain B4567.

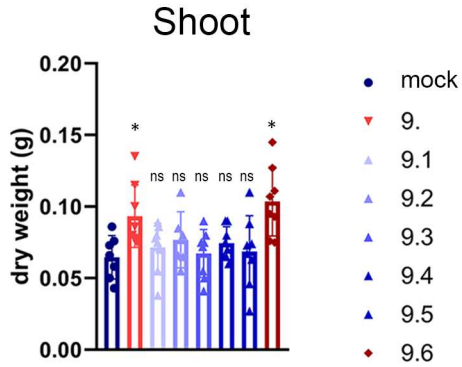
Fig. S7. Effect of bacterial treatment on the photosynthetic performance (F_v/F_m) of tomato leaves under control, drought, and salt stress conditions over time. Mean F_v/F_m values (± SE, $n = 10$) of tomato leaves under control, drought, and salt stress conditions, measured on the indicated days post-inoculation (dpi). No statistically significant differences were observed between treatment groups ($p > 0.05$; linear mixed-effects model followed by Tukey's post hoc test).

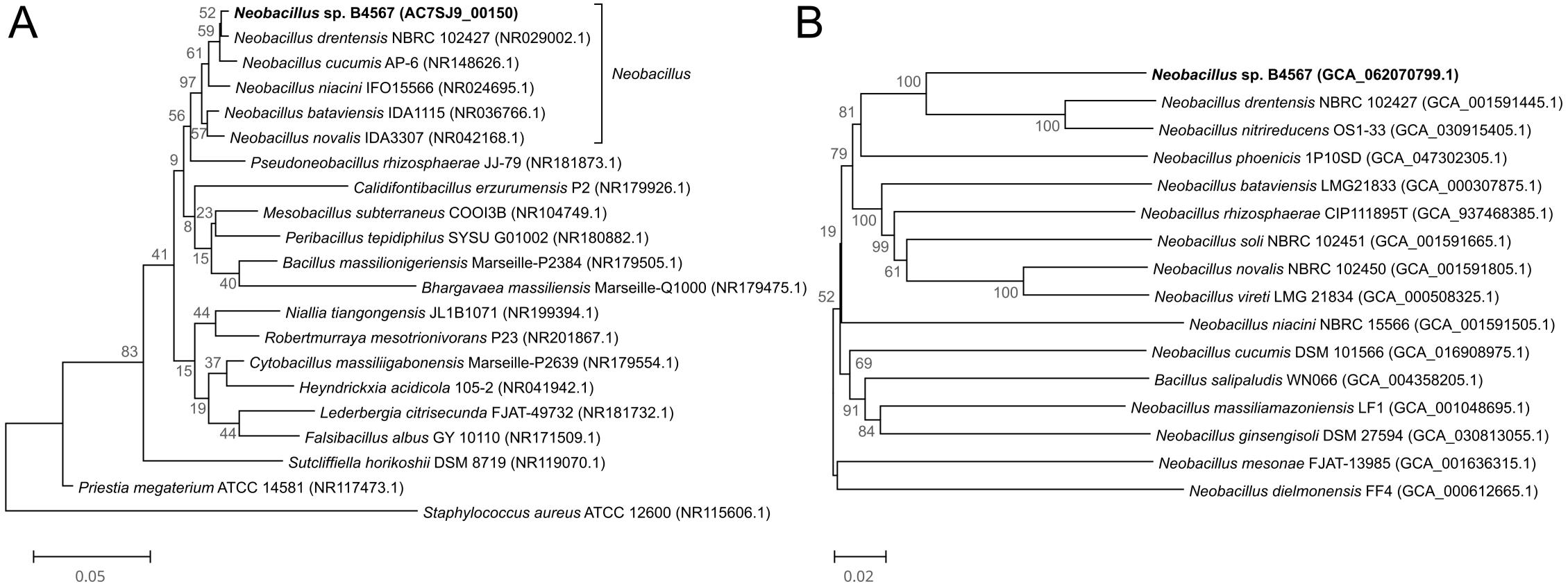

A
B
C

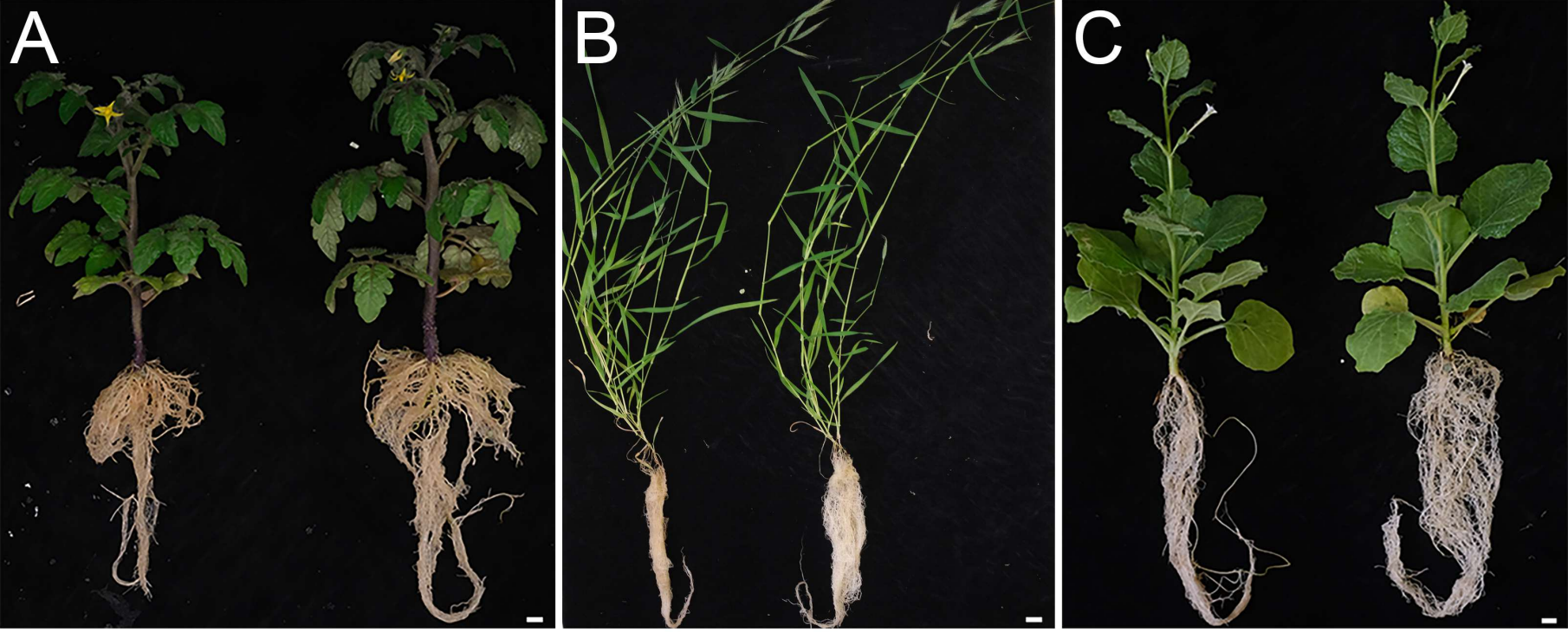
D

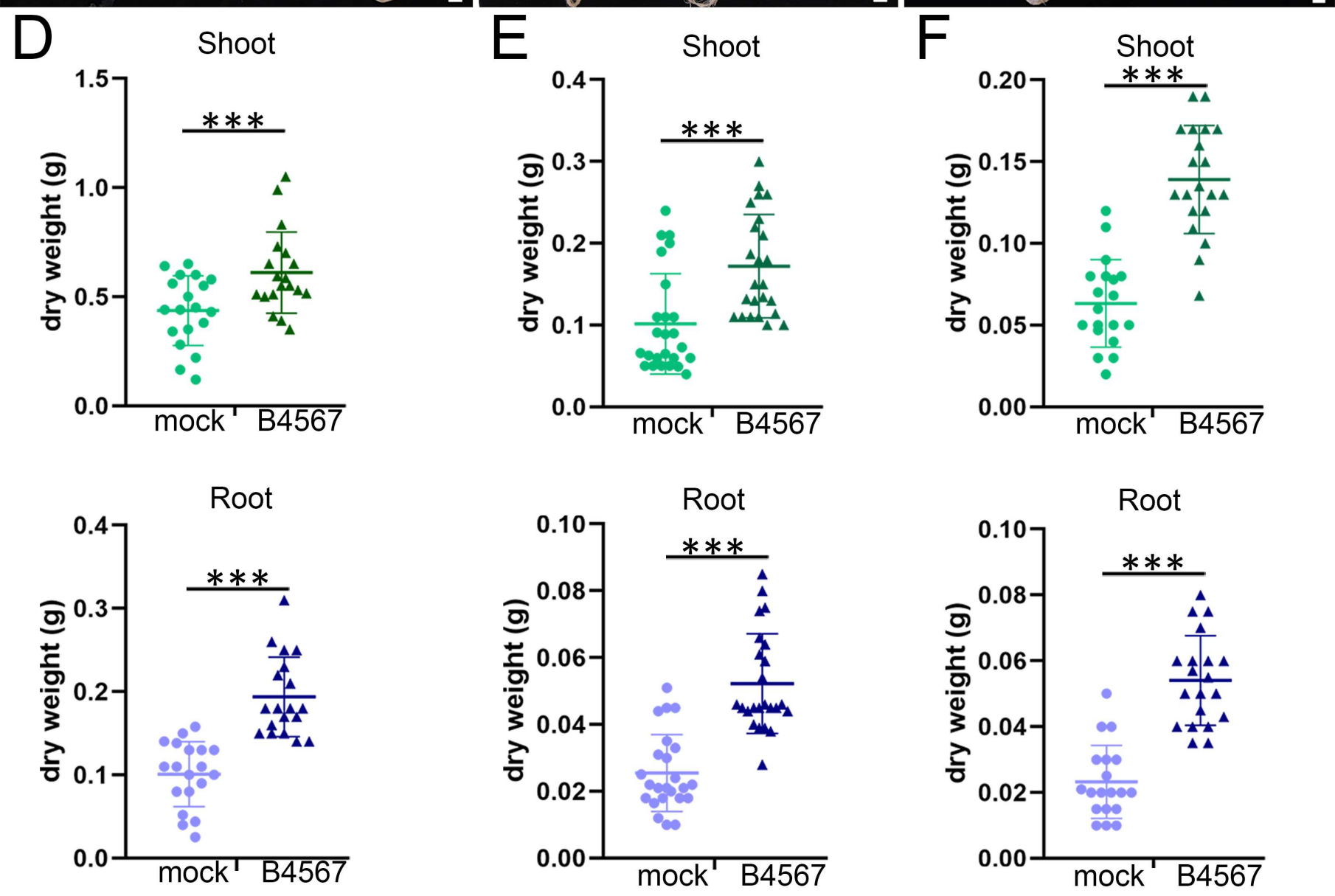

Root
dry weight (g)
0.08
0.06
0.04
0.02
0.00
** ns ns ns * ns **
mock
9.
9.1
9.2
9.3
9.4
9.5
9.6

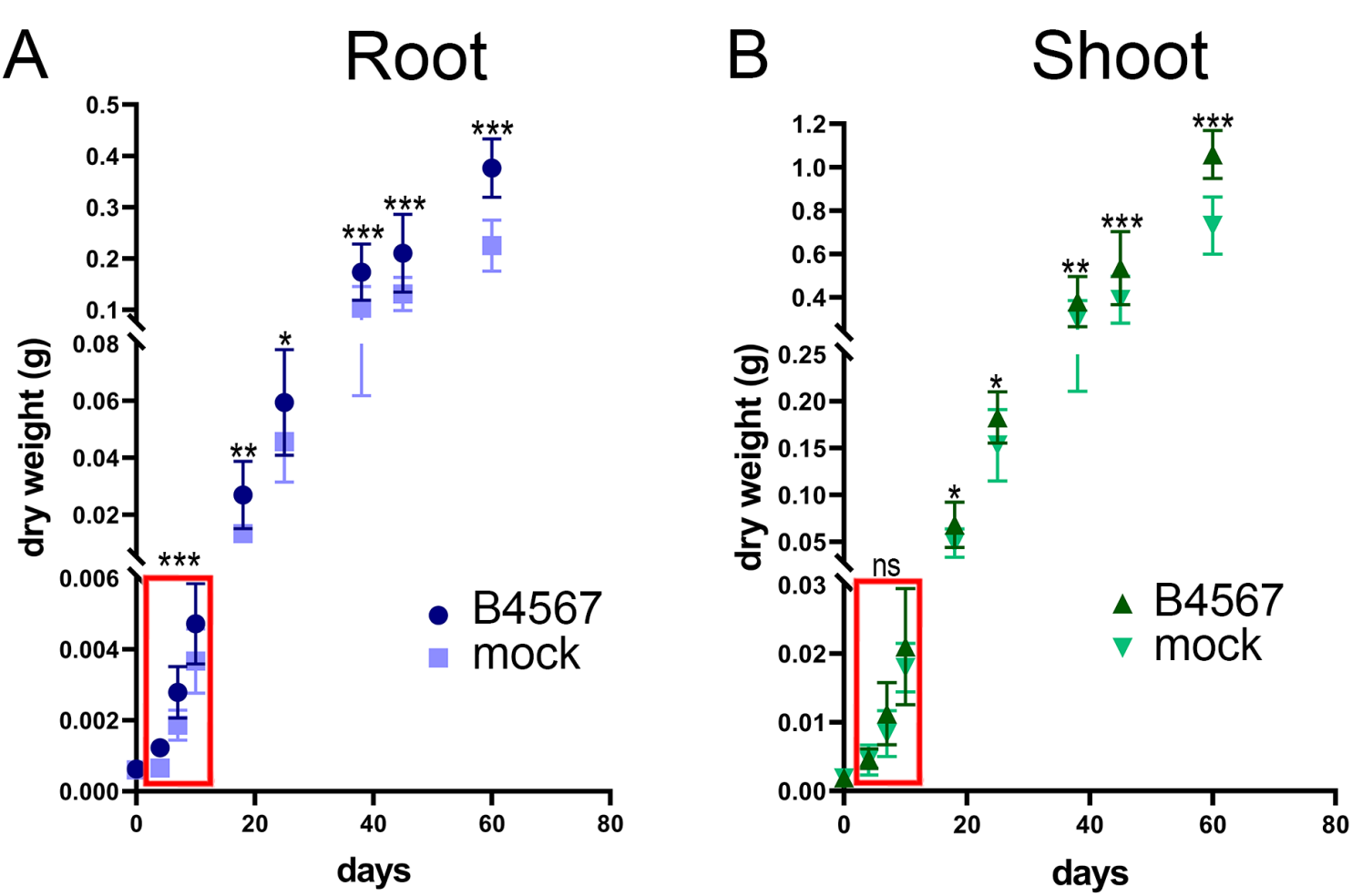
E

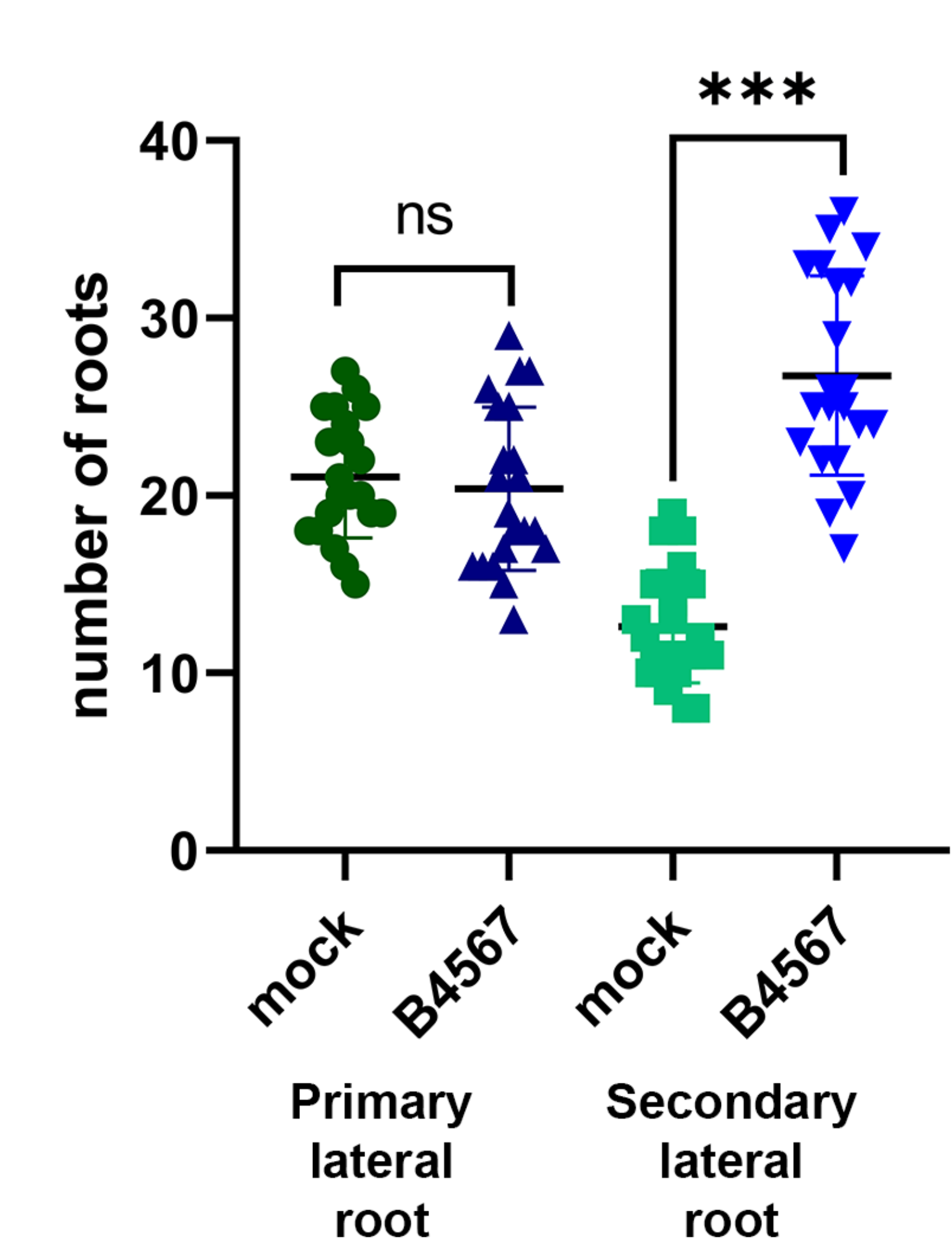

Shoot
dry weight (g)
0.20
0.15
0.10
0.05
0.00
* ns ns ns ns ns *
mock
9.
9.1
9.2
9.3
9.4
9.5
9.6

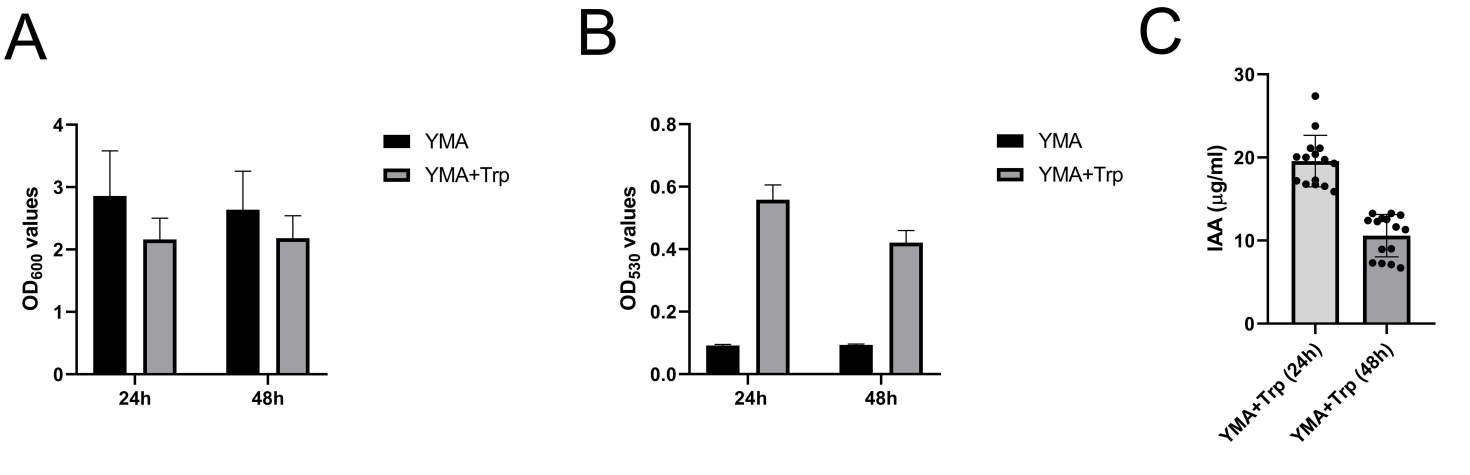

A
52
59
61
97
56
57
9
23
8
15
40
41
44
83
15
37
19
44
Neobacillus sp. B4567 (AC7SJ9_00150)
Neobacillus drentensis NBRC 102427 (NR029002.1)
Neobacillus cucumis AP-6 (NR148626.1)
Neobacillus niacini IFO15566 (NR024695.1)
Neobacillus bataviensis IDA1115 (NR036766.1)
Neobacillus novalis IDA3307 (NR042168.1)
Neobacillus
Pseudoneobacillus rhizosphaerae JJ-79 (NR181873.1)
Calidifontibacillus erzurumensis P2 (NR179926.1)
Mesobacillus subterraneus COOI3B (NR104749.1)
Peribacillus tepidiphilus SYSU G01002 (NR180882.1)
Bacillus massilionigeriensis Marseille-P2384 (NR179505.1)
Bhargavaea massiliensis Marseille-Q1000 (NR179475.1)
Niallia tiangongensis JL1B1071 (NR199394.1)
Robertmurraya mesotrionivorans P23 (NR201867.1)
Cytobacillus massiliigabonensis Marseille-P2639 (NR179554.1)
Heyndrickxia acidicola 105-2 (NR041942.1)
Lederbergia citrisecunda FJAT-49732 (NR181732.1)
Falsibacillus albus GY 10110 (NR171509.1)
Sutcliffiella horikoshii DSM 8719 (NR119070.1)
Priestia megaterium ATCC 14581 (NR117473.1)
Staphylococcus aureus ATCC 12600 (NR115606.1)
0.05
B
100
81
100
79
100
19
99
61
100
52
69
91
84
Neobacillus sp. B4567 (GCA_062070799.1)
Neobacillus drentensis NBRC 102427 (GCA_001591445.1)
Neobacillus nitrireducens OS1-33 (GCA_030915405.1)
Neobacillus phoenicis 1P10SD (GCA_047302305.1)
Neobacillus bataviensis LMG21833 (GCA_000307875.1)
Neobacillus rhizosphaerae CIP111895T (GCA_937468385.1)
Neobacillus soli NBRC 102451 (GCA_001591665.1)
Neobacillus novalis NBRC 102450 (GCA_001591805.1)
Neobacillus vireti LMG 21834 (GCA_000508325.1)
Neobacillus niacini NBRC 15566 (GCA_001591505.1)
Neobacillus cucumis DSM 101566 (GCA_016908975.1)
Bacillus salipaludis WN066 (GCA_004358205.1)
Neobacillus massiliamazoniensis LF1 (GCA_001048695.1)
Neobacillus ginsengisoli DSM 27594 (GCA_030813055.1)
Neobacillus mesonae FJAT-13985 (GCA_001636315.1)
Neobacillus dielmonensis FF4 (GCA_000612665.1)
0.02

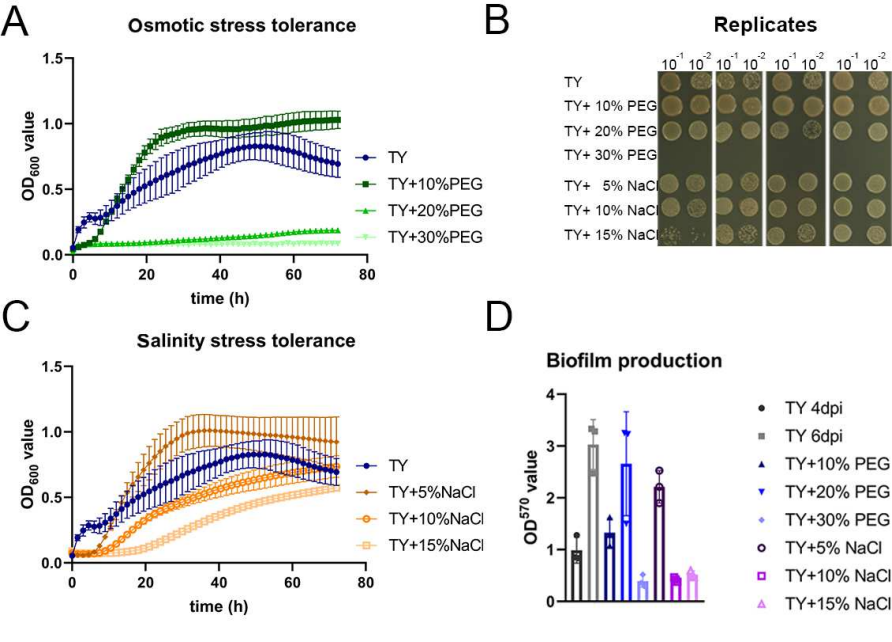

A
B
C

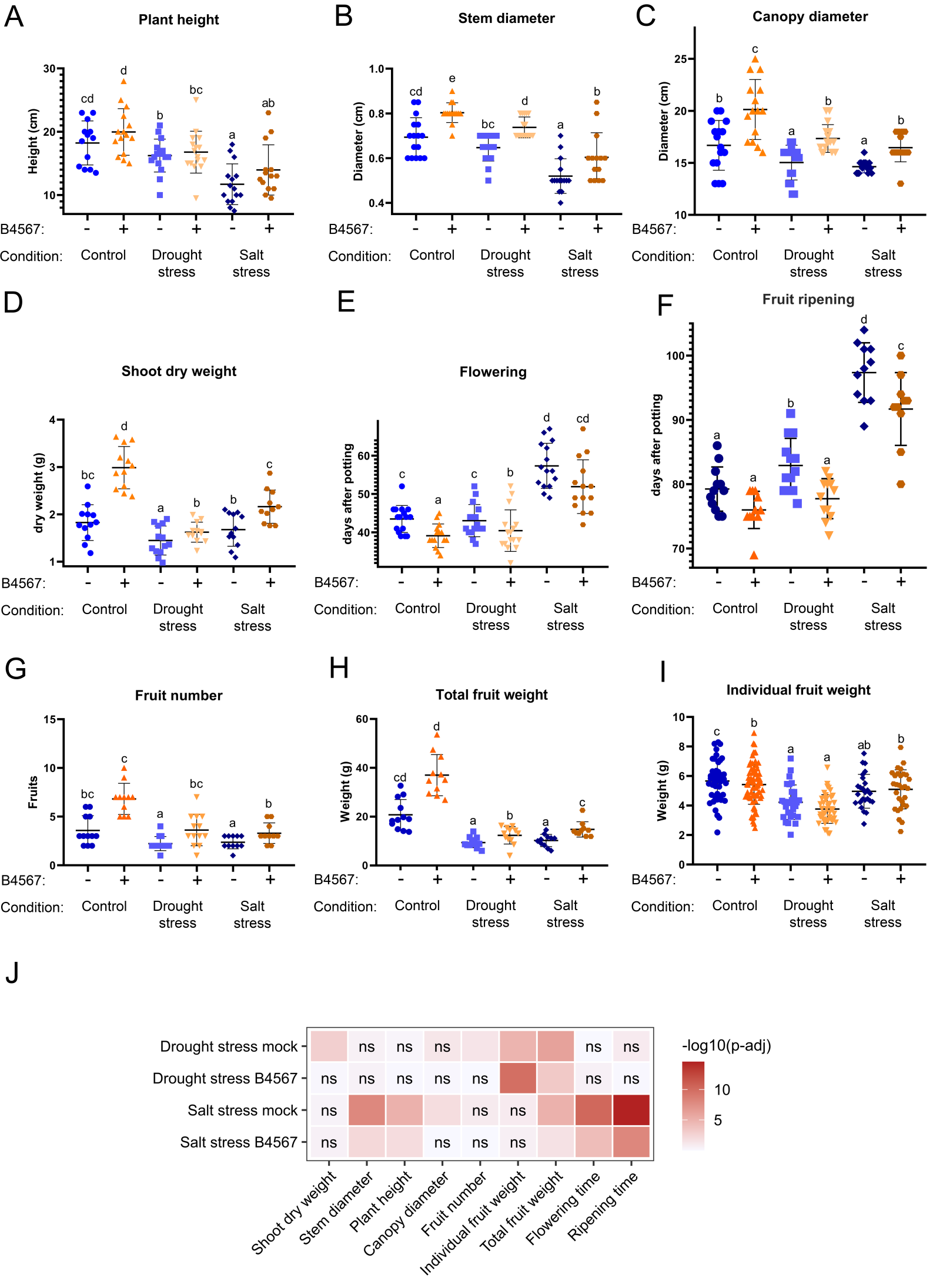

D
Shoot
dry weight (g)
1.5
1.0
0.5
0.0
***
mock
B4567
E
Shoot
dry weight (g)
0.4
0.3
0.2
0.1
0.0
***
mock
B4567
F
Shoot
dry weight (g)
0.20
0.15
0.10
0.05
0.00
***
mock
B4567
Root
dry weight (g)
0.4
0.3
0.2
0.1
0.0
***
mock
B4567
Root
dry weight (g)
0.10
0.08
0.06
0.04
0.02
0.00
***
mock
B4567
Root
dry weight (g)
0.10
0.08
0.06
0.04
0.02
0.00
***
mock
B4567


A
Root
B
Shoot
dry weight (g)
days
B4567
mock
ns
*
**
***


***
ns
40
30
20
10
0
number of roots
mock
B4567
mock
B4567
Primary lateral root
Secondary lateral root


A
B
C
OD600 values
OD530 values
IAA (μg/ml)
YMA
YMA+Trp
24h
48h
YMA+Trp (24h)
YMA+Trp (48h)


A
Osmotic stress tolerance
OD600 value
time (h)
TY
TY+10%PEG
TY+20%PEG
TY+30%PEG
B
Replicates
TY
TY+ 10% PEG
TY+ 20% PEG
TY+ 30% PEG
TY+ 5% NaCl
TY+ 10% NaCl
TY+ 15% NaCl
C
Salinity stress tolerance
OD600 value
time (h)
TY
TY+5%NaCl
TY+10%NaCl
TY+15%NaCl
D
Biofilm production
OD570 value
TY 4dpi
TY 6dpi
TY+10% PEG
TY+20% PEG
TY+30% PEG
TY+5% NaCl
TY+10% NaCl
TY+15% NaCl


A
Plant height
Height (cm)
B
Stem diameter
Diameter (cm)
C
Canopy diameter
Diameter (cm)
D
Shoot dry weight
dry weight (g)
E
Flowering
days after potting
F
Fruit ripening
days after potting
G
Fruit number
Fruits
H
Total fruit weight
Weight (g)
I
Individual fruit weight
Weight (g)
B4567:
Condition:
Control
Drought stress
Salt stress
J
Drought stress mock
Drought stress B4567
Salt stress mock
Salt stress B4567
Shoot dry weight
Stem diameter
Plant height
Canopy diameter
Fruit number
Individual fruit weight
Total fruit weight
Flowering time
Ripening time
-log10(p-adj)
10
5

Test	PGP function	Results	Summary
Pikovskaya's agar test	Phosphor mobilization	negative	-
Blue Agar CAS assay	Siderophore production	negative	-
IAA test	Auxin production	19 μg/ml production	++
ACC deaminase test	Reduction of ethylene level	negative	-
Growing in 10–30% PEG cc.	Osmotic stress tolerance	tolerates 20% PEG	+
Growing in 5–15% NaCl cc.	Salinity stress tolerance	tolerates 15% NaCl	++
Biofilm production	Enhances colonization	moderate production	+

Supplementary Files

This is a list of supplementary files associated with this preprint. Click to download.

- NeobacillusPGPRmanuscriptfinalv3withtrackchanges.docx
- SupplementaryFigures.pdf